EUROPEAN JOURNAL OF PURE AND APPLIED MATHEMATICS
2025, Vol. 18, Issue 3, Article Number 6517
ISSN 1307-5543 – ejpam.com
Published by New York Business Global

Numerical and Statistical Sensitivity Analysis of Deterministic and Stochastic SVEITR Model for Measles Infection

Madhia Mohiudin[1,*], Sana Ullah[2], Shema Khan[3], Naveed Ahmad[4], Sadique Ahmad[4], Mohammed A. Elaffendi[4]

[1] *Department of Mathematics, COMSATS University Islamabad, Islamabad Campus, Park Road, Tarlai Kalan, Islamabad 45550, Pakistan*
[2] *Department of Mathematics, University of Malakand, Chakdara Dir(L), 18000, Khyber Pakhtunkhwa, Pakistan*
[3] *Department of Mathematics, Government Post Graduate Jahanzeb College, Swat, KPK, Pakistan*
[4] *IAS Data Science and BlockChain Laboratory, College of Computer and Information Sciences, Prince Sultan University, Riyadh 11586, Saudi Arabia*

Abstract. Measles is a global health concern due to its high contagiousness and rapid transmission, especially in low-vaccination areas. This article uses an SVEITR model to explain measles transmission and control dynamics. The model is stable at two equilibria and can be verified using the Non-Standard Finite Difference (NSFD) technique. The study offers valuable advice to public health professionals and legislators working to prevent and manage measles, highlighting the importance of international cooperation and vaccination in preventing the disease's return.

2020 Mathematics Subject Classifications: 92D30, 34D20, 60H10, 65L12

Key Words and Phrases: Statistical sensitivity analysis, Basic reproduction number, Global stability, Lyapunov function, Stochastic SVEITR model

1. Introduction

Measles is an extremely transmissible virus that has remained a major worldwide health problem in spite of medical science improvements. Measles, which is characterized by a characteristic rash and influenza-like symptoms, is a serious concern, especially in places with poor vaccination rates and limited access to healthcare [1]. Respiratory droplets are

*Corresponding author.
DOI: https://doi.org/10.29020/nybg.ejpam.v18i3.6517

Email addresses: madhia.mohiudin@gmail.com (M. Mohiudin), safi1987maths@gmail.com (S. Ullah), shemakhan805@gmail.com (S. Khan), nahmed@psu.edu.sa (N. Ahmad), saahmad@psu.edu.sa (S. Ahmad), affendi@psu.edu.sa (M. A. Elaffendi)

the main way that the Measles virus (MeV), which causes the viral infection, is spread. Its high contagiousness is highlighted by the fact that an infected person might spread the illness to others before symptom manifest. Measles, which is spread by inhaling air polluted by asymptomatic individuals or by coming into contact with contagious respiratory or swallowing secretions (things like coughing or sneezing), is one of the most widely transmitted contagious diseases in the world. For as long as two hours, the virus can be spread through the atmosphere or on contaminated surfaces. Because of this, measles is extremely contagious, and an infected individual can spread the disease to nine among ten of their close, unvaccinated acquaintances. An infected person can spread it between four days before the rash appears and four days after it does. Outbreaks of measles can cause serious complications and even death, particularly in young, undernourished children. In nations nearing measles eradication, imported cases continue to be a significant source of infection. Measles may spread quickly, which makes it a powerful outbreak agent, particularly in areas with high population density [2, 3]. The first signs of a measles infection appear after an incubation time frame of roughly 10 to 14 days. Red, watery eyes, a runny nose, coughing, a severe temperature, and a body rash are common symptoms. The trait Measles rash usually starts on the neck and face and spreads down the body 7-18 days later contact [4]. It often fades after 5-6 days. After infecting the respiratory system, the measles virus progresses throughout the body. Although it can infect anyone, children are more frequently infected with the measles virus. Complications can occur, even though most people recover in a few weeks, particularly in susceptible groups such small children, pregnant women, and those with compromised immune systems. Women who contract measles during pregnancy run the risk of harming themselves and giving birth to a preterm, underweight child. Measles can cause serious complications, such as brain inflammation, pneumonia, blindness, severe diarrhea and associated dehydration, infections of the ears, severe respiratory issues, and even death [5]. Complications are expected to affect children under five and adults over thirty. They are more common in malnourished youngsters, especially those whose don't get enough vitamin A or which have compromised immune systems because of HIV or other diseases. Since measles itself weakens immunity and might make the body lose how to fight off illnesses, children are especially vulnerable. Since vaccinations can largely prevent measles-related deaths, immunization campaigns are essential to halting the disease's spread.

Since measles itself weakens immunity and might make the body lose how to fight off illnesses, children are especially vulnerable. Immunization campaigns are crucial to stopping the spread of measles since immunizations can significantly reduce the number of deaths caused by the illness. A safe and efficient method of establishing immunity for the virus is the measles vaccination, which is frequently given as a component of the rubella-mumps-Measles (RMM) vaccine [6, 7]. In many regions of the world, extensive vaccination campaigns have resulted in a notable decline in cases of measles and fatalities. To stop outbreaks and keep disease under control, high immunization rates must be maintained. When communities achieve high vaccination coverage, particularly with a two-dose regimen, they can create herd immunity, which provides additional security to those who cannot receive vaccinations for medical reasons [8, 9]. Many nations and

international health organizations aim to eradicate measles. It will take consistent work to achieve eradication, including making sure vaccines are accessible, bolstering healthcare systems, and combating vaccine reluctance and disinformation. Given how quickly measles can spread across borders, international cooperation and coordination are crucial. Despite advancements, difficulties still exist. Measles control efforts may be hampered by vaccine hesitancy, which occurs when people postpone or refuse immunization even though they have access to it [10, 11]. Measles outbreaks have been made possible by pockets of unvaccinated people who have been influenced by false information on vaccines and their safety. Due to limited outbreaks and a return of cases in certain locations, measles has received fresh attention in recent years. These occurrences highlight the significance of aggressive immunization campaigns and ongoing attention [12].

Every child ought to have a measles vaccination. The vaccination is affordable, safe, and effective. To guarantee immunity, children must get two doses of the vaccination. In nations where measles is prevalent, the first dosage is often administered at nine months of age; in other nations, it is given between 12 and 15 months. Later in childhood, often between 15 and 18 months, a second dosage should be administered. The measles vaccine is administered either by itself or frequently in conjunction with the varicella, mumps, and rubella vaccines. Reducing the number of measles deaths worldwide requires both routine vaccination and major immunization programs in nations with high case rates. For less than $1USD$ per child, the measles vaccine remains in use for almost 60 years. In an emergency, the measles vaccine also serves to prevent the spread of outbreaks. Refugees are more vulnerable to measles epidemics, so they should get vaccinated as quickly as feasible [13]. Combining vaccines gives a boost of immunity of rubella, a particularly common vaccine-preventable disease that may infect unborn children, while also allowing for pooled delivery and administration costs. About 83% of children worldwide received one dose of the measles vaccine before the time of their first birth, and 74% of infants received both doses in 2022 [14]. Since not all children gain immunity after the first dose, two boosters of the vaccination are advised to guarantee immunity and stop outbreaks. In 2022, almost 22 million babies did not receive at least one dose of the measles vaccination as part of their regular immunization schedule. Measles does not have a specific therapy. The goals of care should be to reduce symptoms, ensure the patient is comfortable, and avoid complications. Fluids lost due to vomiting or diarrhea can be replaced by drinking adequate water and receiving dehydration treatments. Consuming a nutritious diet is also crucial. Antibiotics are sometimes prescribed by doctors to treat ears and eye infection as well as pneumonia. Vitamin A supplements should be administered in two doses, separated by 24 hours, to all children and adults who have measles. This raises the vitamin's levels that are low, even in youngsters who are fed a healthy diet. It can aid in preventing blindness and eye damage. Supplementing with vitamin A may help lower the incidence of measles deaths.

A key approach for examining the dynamics of disease transmission within communities is mathematical modeling of pandemics, which makes use of computational simulations and mathematical equations [7, 15]. These models enable public health professionals make well-informed decisions by illustrating the interactions between vulnerable, recovered, and

infected individuals. This gives them insights into how illnesses propagate. These models forecast how an epidemic will develop by taking into account a number of variables, including population size, transmission rates, and response tactics. They are able to predict when peak cases will occur, the possible number of infections, and the effects of various control strategies. Sensitivity analysis finds important parameters that affect results and aids in evaluating the model's robustness. Furthermore, mathematical modeling has played a critical role in guiding the implementation of measures like lockdowns, testing, and vaccination campaigns in response to epidemic outbreaks. Models are still essential resources for comprehending epidemics and creating successful treatments to safeguard public health, despite their limitations brought on by uncertainties and simplifications [16]. Analyzing the effects of vaccine hesitancy, taking into account geographical considerations for limited pandemics, and dealing with the connection between measles and other illnesses within large epidemiological networks have been the main focuses of recent advances in mathematical simulation of measles [17].

A mathematical approach called optimal control theory, when applied to epidemic models, seeks to determine the best ways to stop the spread of infectious illnesses inside the community [17–19]. The theory aims to ascertain the best way to distribute resources, including vaccination campaigns, quarantine policies, medication transportation, and various other public health initiatives, by using mathematical models that illustrate the dynamics of disease transmission. This entails developing a mathematical function of objective variables that measures the expenses related to the effects of the disease and the use of preventative interventions. Then, over time, the control variables-which stand in for the interventions-are modified to minimize the desired function while respecting realistic restrictions like financial and resource constraints. By taking into account both epidemiological dynamics and pragmatic factors, optimum theory of control [20] offers decision-makers a methodical and mathematical system for proactively managing epidemics. Furthermore, sensitivity evaluation and measurement of uncertainty are being used in optimal control studies to deal with the inherent risk in disease models [21, 22]. This makes it easier to comprehend how resilient control techniques are to different situations and parameter uncertainty. Optimal control measures today frequently incorporate thorough cost-benefit analysis in addition to minimizing illness burden. This means assessing how different solutions will affect the economy in terms of medical expenses, lost output, and intervention costs. By taking into account both financial and health outcomes, this method helps policymakers make well-informed decisions [23–25].

Measles continues to pose a concern to world health because of its high contagiousness and quick dissemination, particularly in places having low immunization rates. The high frequency of cross-border transmission emphasizes how urgently worldwide vaccination and concerted efforts to stop epidemics are needed. The ultimate goal is to contribute to the possible eradication of measles by creating efficient disease management systems. The goal of this study is to improve knowledge about measles control and transmission. Thus, a thorough investigation of viral transmission dynamics, with an emphasis on comprehending, controlling, and improving control methods, serves as the driving force behind the study. The goal of the study is to make a significant contribution to the fields of pub-

lic health policy and infectious disease modeling. The project is to support international health initiatives and policies targeted at avoiding and managing measles outbreaks by evaluating the efficacy of various control tactics, such as continuous measures and optimal interventions. Enhancing our knowledge of measles behavior and offering evidence-based suggestions for better disease management globally are the ultimate goals. A research team recently created an SEIR Measles simulation [26], which was released in 2019. Their goals were to conduct numerical simulations to examine the evolution of Measles disease in the future and to assess the model's existence, uniqueness, and local stability in a disease-free state only. But there are several problems with their strategy. For instance, they employed a selectively converging RK4 numerical scheme to confirm their analytical conclusions, carried out an insufficient sensitivity analysis, and failed to demonstrate the models global and local asymptotic processes at its equilibrium states. Measles can be eliminated from the human population, but their study doesn't show how or by what means. It is essential to comprehend how interventions can affect the dynamics of measles in order to influence public health policies. It would be beneficial to encourage the researchers to investigate other well-thought-out intervention options, such vaccination campaigns or restrictions on quarantine and therapy, and to assess how well they work to control or eradicate measles from the human population. In order to examine the long-term dynamics of measles disease, we developed an expanded SVEITR model in the current study by including therapy and vaccination compartments [26]. Those that are infected are referred to treatment, where they are segregated or given the necessary medical attention. In the meanwhile, those with strong immune systems can heal themselves without medical intervention. In situations where there is still a possibility of exposure for vaccinated persons due to an incomplete vaccine, susceptible individuals are vaccinated. We extended the model [26] and showed its existence and uniqueness, key properties, and both global and local hyperbolic stability at its equilibrium states in order to make the problem well-posed. To evaluate the effect of the various parameters on the spread of the disease, sensitivity analysis is also carried out. In order to compare the deterministic and stochastic numerical simulations, we also transform the deterministic model to the stochastic model. The comparison demonstrates the relationship between the dynamics and how they change over time. There are ten sections in the manuscript. We developed a dynamic deterministic measles model in Section 2 and evaluated a number of its qualitative biological characteristics. We have demonstrated that there is a unique, positive, and bounded solution in order to establish epidemiologic significance, making the problem clearly specified in Sect. 3. The model's identification with both disease-free and epidemic equilibrium states was crucial to understanding the long-term behavior of the illness. The numerical value of the threshold factor is calculated using the next-generation approach in section 4. The model's local and global stable at its equilibria was established by a thorough stability study, with the threshold number subjected to the required circumstances. Nonetheless, Lyapunov theory was used to demonstrate global stability in section 5. The model's sensitivity analysis is shown in section 6, and the deterministic model's numerical analysis is presented in section 7. Section 8 presents the deterministic model in its stochastic form, while Section 9 presents its numerical simulation. The conclusion of the entire book is

presented in the last section.

2. Formulation of the Model

Numerous papers have detailed a number of mathematical models to examine the dynamics behind the spread of measles [27–31]. These models are useful in a variety of epidemiological fields and are essential for aiding public health planners and policymakers in their decision-making processes. The underlying evolution of infectious diseases like measles, transmission patterns, and the possible effects of public health measures are all better understood by mathematical modeling [32, 33]. In order to assess interventions, plan studies, and contain epidemic outbreaks, modeling has become more and more important. In addition to helping with the testing and development of important theories, epidemiological models [34, 35] offer a conceptual grasp of how diseases propagate. These models aid in the creation of hypotheses, the validation of experimental designs, the interpretation of results, the derivation of diagnoses from observable symptoms and indications, the support of decision-making, and the validation of findings [36]. In essence, modeling is a crucial statistical tool in the continuous fight against infectious illnesses, including measles.

In order to examine the variations in measles transmission, we have developed a novel real-world $\mathbb{SEITR}$ model in this study. Assessing the effectiveness of vaccination and treatment plans in preventing the spread of measles, both before and after optimization stages, is our main goal. It is important to emphasize that the foundation of our concept is the idea that vaccination tactics are not infallible. This indicates that it takes into account the chance that individuals may be re-susceptible throughout the vaccine period, which could result interesting dynamic. Additionally, it takes into consideration the chance that some people may end up healthy and unaffected before treatment. Our research enables us to investigate the effects of treatment and immunization plans in real-world scenarios, when it might not be possible to achieve 100% vaccine coverage. We believe that our research will greatly advance our knowledge of practical strategies for halting the spread of measles. All things considered, our research tackles a significant public health issue and seeks to offer insightful information about the mechanisms of measles spread and the efficacy of intervention techniques in practical settings. There are six different compartments for the entire population, denoted by $\mathbb{M}(t)$. A healthy individual who runs the danger of getting sick after coming into contact with an infected person is said to be susceptible $\mathbb{S}(t)$ represents the first class. The second class, known as the vaccinated class or $\mathbb{V}(t)$, is made up of healthy people who have been vaccinated to lessen their vulnerability to the illness. The next compartment, known as the exposed class and represented by $\mathbb{E}(t)$, is made up of exposed people. The exposed persons are those who are infected and, while they may or may not exhibit symptoms, are unable to transmit others. People who are at present infectious and able to infect others are included in the fourth class, denoted by $\mathbb{I}(t)$, sometimes known as the infected class. Those receiving medical treatment are included in the fifth class, represented by $\mathbb{T}(t)$, which is referred to as the treatment class. Lastly, the sixth group, designated $\mathbb{R}(t)$, also known as the recovered class, is made up

of people who have been cured of the illness by therapy or vaccination and are unable to contract it again. The total population is taken as

$$\mathbb{M}(t) = \mathbb{S}(t) + \mathbb{V}(t) + \mathbb{E}(t) + \mathbb{I}(t) + \mathbb{T}(t) + \mathbb{R}(t).$$

New people joining the susceptible class is happening at b rate. A common approach to depict the frequency of infection spread from susceptible to people who are exposed due to interaction with infected individuals is to use the strength of disease, which is represented by the symbol k. In essence, it is a measurement of the likelihood of transmission for each interaction between an infectious person and a susceptible person. The frequency with which susceptible people are immunized to develop disease immunity is indicated by the metric c_2. The μ_0 represents the intrinsic rate of death in the susceptible group, while c_1 are re-susceptible rate. Thus, the overall pace of transformation of those who are most susceptible can be expressed as

$$\frac{d\mathbb{S}(t)}{dt} = b + c_1\mathbb{V} - \frac{k\mathbb{S}\mathbb{I}}{\mathbb{M}} - (c_2 + \mu_0)\mathbb{S}.$$

Vaccinated people may become susceptible because of their compromised immunity or other reasons, and they will then move to the exposed compartment $\mathbb{E}(t)$ at the amount represented by c_1. Recruitment of new individuals from the susceptible compartment $\mathbb{S}(t)$ to the vaccinated class occurs at a rate of c_2. μ_0 is a representation of the vaccination compartment natural mortality rate. The following is the net rate of change for those who have received vaccinations,

$$\frac{d\mathbb{V}(t)}{dt} = c_2\mathbb{S} - (c_1 + \mu_0)\mathbb{V}.$$

k represent the susceptible compartment contribute additional members to the compartment of exposed individuals. α shows the pace at which members of this exposed compartment migrate to the infected compartment. r_1 is the recovering rate for people in the exposed compartment. Additionally, the rate μ_0 indicates a departure from the exposed compartment because of natural death. The usual differential equation describes the total change in the number of people in the exposed group as,

$$\frac{d\mathbb{E}(t)}{dt} = \frac{k\mathbb{S}\mathbb{I}}{\mathbb{M}} - (\alpha + r_1 + \mu_0)\mathbb{E}.$$

At a rate of α, new members of the infectious class are recruited by the exposed compartment. At a rate of θ, those in the infectious group who are severely afflicted are sent for treatment. The natural death rate is shown by μ_0, while the infection death rate denoted by d_1. Consequently, the net rate of change of people within the infectious class is taken into consideration using the following equation,

$$\frac{d\mathbb{I}(t)}{dt} = \alpha\mathbb{E} - (\theta + d_1 + \mu_0)\mathbb{I}.$$

Infectious individuals enter the treatment compartment at θ, and go to the recovered compartment at r_2. The rate of natural death causes an leave from the therapy compartment

at μ_o, while the death rate during treatment is by d_2. Consequently, the following formula represents the net variation in the treatment compartment,

$$\frac{d\mathbb{T}(t)}{dt} = \theta\mathbb{I} - (r_2 + d_2 + \mu_0)\mathbb{T}.$$

Accordingly, r_1 and r_2 represent the transmission rates from the treatment and exposed compartment to the recovered compartment. Due to the natural death rate μ_0, some people leave the recovered class. The formula that determines the total rate of change for people in the recovered compartment over time is hence

$$\frac{d\mathbb{R}(t)}{dt} = r_2\mathbb{T} + r_1\mathbb{E} - \mu_0\mathbb{R}.$$

To demonstrate the dynamics of measles, we develop a thorough mathematical model by integrating all of the previously discussed differential equations.

$$\begin{aligned}
\frac{d\mathbb{S}(t)}{dt} &= b + c_1\mathbb{V} - \frac{k\mathbb{S}\mathbb{I}}{\mathbb{M}} - (c_2 + \mu_0)\mathbb{S},\\
\frac{d\mathbb{V}(t)}{dt} &= c_2\mathbb{S} - (c_1 + \mu_0)\mathbb{V},\\
\frac{d\mathbb{E}(t)}{dt} &= \frac{k\mathbb{S}\mathbb{I}}{\mathbb{M}} - (\alpha + r_1 + \mu_0)\mathbb{E},\\
\frac{d\mathbb{I}(t)}{dt} &= \alpha\mathbb{E} - (\theta + d_1 + \mu_0)\mathbb{I},\\
\frac{d\mathbb{T}(t)}{dt} &= \theta\mathbb{I} - (r_2 + d_2 + \mu_0)\mathbb{T},\\
\frac{d\mathbb{R}(t)}{dt} &= r_2\mathbb{T} + r_1\mathbb{E} - \mu_0\mathbb{R}.
\end{aligned} \tag{1}$$

Subject to the initial condition:

$$\mathbb{S}(0) \geq 0, \mathbb{V}(0) \geq 0, \mathbb{E}(0) \geq 0, \mathbb{I}(0) \geq 0, \mathbb{T}(0) \geq 0, \mathbb{R}(0) \geq 0.$$

The model is displayed in the form of flow chart as follows:

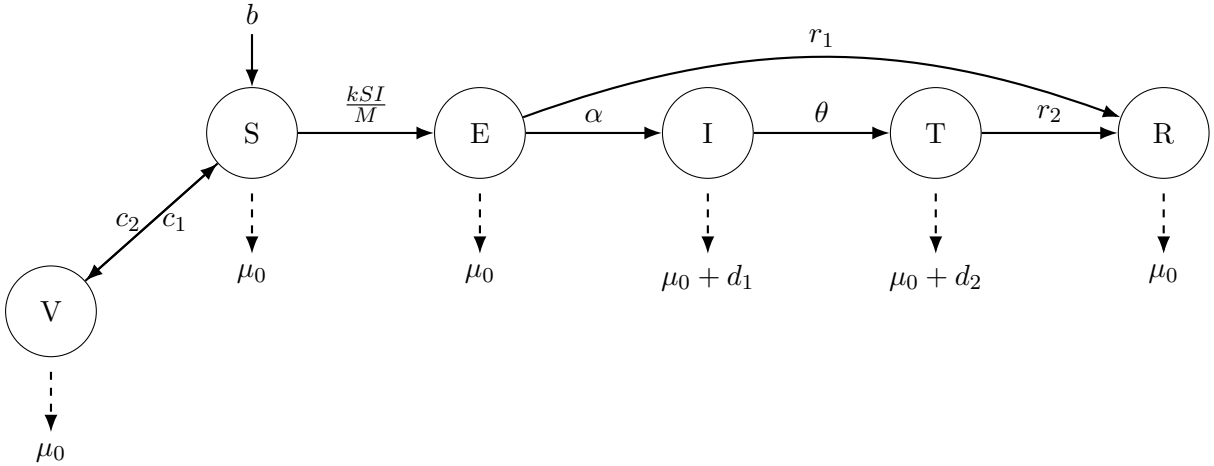

3. Mathematical Analysis

This section covers the model (1) characteristics, including the solution's boundedness, positivity, and well-posedness $t \geq 0$.
Let $y : [0 \to \infty) \implies \mathcal{R}^6$ be provide by $y = (\mathbb{S} + \mathbb{V} + \mathbb{E} + \mathbb{I} + \mathbb{T} + \mathbb{R})^T$ a vector common in $\mathcal{R}^6$ comprising six state parameters. Let $g(y) = (g_1(y) + g_2(y) + g_3(y) + g_4(y) + g_5(y) + g_6(y))^T$ be provided by $g : \mathcal{R}^6 \implies \mathcal{R}^6$, a function with a vector value defined by $\mathcal{R}^6$ where

$$\begin{aligned} g_1(y) &= b + c_1\mathbb{V} - \frac{k\mathbb{S}\mathbb{I}}{\mathbb{M}} - \mu_0\mathbb{S} - c_2\mathbb{S}, \\ g_2(y) &= c_2\mathbb{S} - c_1\mathbb{V} - \mu_0\mathbb{V}, \\ g_3(y) &= \frac{k\mathbb{S}\mathbb{I}}{\mathbb{M}} - \alpha\mathbb{E} - r_1\mathbb{E} - \mu_0\mathbb{E}, \\ g_4(y) &= \alpha\mathbb{E} - \theta)\mathbb{I} - (d_1 + \mu_0)\mathbb{I}, \\ g_5(y) &= \theta\mathbb{I} - r_2\mathbb{T} - (d_2 + \mu_0)\mathbb{T}, \\ g_6(y) &= r_2\mathbb{T} + r_1\mathbb{E} - \mu_0\mathbb{R}. \end{aligned} \tag{2}$$

In compact form, the system (1) − (2) can be expressed as:

$$\frac{d\mathbf{x}}{dt} = \mathbb{G}(y), x(0) = x_0 \tag{3}$$

Here $x_0 = (\mathbb{S}(0), \mathbb{P}(0), \mathbb{I}(0), \mathbb{T}(0), \mathbb{R}(0))^T$

Theorem 1. *The function $\mathbb{G}$ is continuous Lipschitly in y.*

Proof. As six state variable, ($\mathbb{S}, \mathbb{V}, \mathbb{E}, \mathbb{I}, \mathbb{T}$ and $\mathbb{R}$) are continuous differentiable equations of t and hence are the elements, $g_1(y), g_2(y), g_3(y), g_4(y)$, $g_5(y)$ and $g_6(y)$ of the function $\mathbb{G}$. Let assume, $\mathbb{L}(y, z, b) = x + b(z - y) : b \in [0, 1], y, z \in \mathcal{R}^6$. A set $\mathbb{L}(y, z, b)$ is a section of a line in $\mathcal{R}^6$ which meets the point y to z as b varies from 0 to 1, and is a compact subset of $\mathcal{R}^6$. Therefore, we can select a point $c \in \mathbb{L}(y, z, b)$ so that the subsequent equalities hold by using the Mean Value Theorem,

$$\|\mathbb{G}(z) - \mathbb{G}(y)\|_\infty = \|\mathbb{G}'(c; z - y)\|_\infty \tag{4}$$

Here $\mathbb{G}(c; z - y)$ is a directional derivatives of the function $\mathbb{G}$ at c in the direction of z-y. So, we have

$$\|\mathbb{G}'(c; z - y)\|_\infty = \sum_{i=1}^{6} \|\mathbf{J}g_i(z).(z - y)e_i\|_\infty \leq \sum_{i=1}^{6} \|\mathbf{J}g_i(z)\|_\infty \|z - y|_\infty.$$

The abounded linear operator $\mathbf{J}g_i(c)$ and the i^{th} coordinate unit column e_i in $\mathcal{R}^6_+$ are used here. Given the limited nature of the partial derivatives of the function $g_i, i = 1, 2, 3, 4, 5, 6$, there exists an integer K_1 such that,

$$\sum_{i=1}^{6} \|\mathbf{J}g_i(z)\|_\infty \leq K_1,$$

for $c \in \mathbb{L}(y, z, b) \subseteq \mathcal{R}_+^6$. Consequently, we have

$$\|\mathbb{G}(z) - \mathbb{G}(y)\|_\infty \leq K_1 \|z - y|_\infty,$$

and so its prove that $\mathbb{G}$ is Lipschitz continuous.

Theorem 2. *The system (4) has a unique solution.*

Proof. According to Theorem 1, a system $\mathbb{G}$ presented in (4) is Lipschitz continuous in y. Thus, the system (4) has a unique solution according to the Picard theorem of existence and uniqueness. It is considered practical if the system solution (1), or equivalently (4), is bounded and nonnegative. Since the values of a realistic solution may be determined by gathering data, it is physically dependable.

Theorem 3. *In $\mathcal{R}_+^6$, the nonlinear system (1) contains a global solution ($\mathbb{S}, \mathbb{V}, \mathbb{E}, \mathbb{I}, \mathbb{T}$, $\mathbb{R}$) for any nonnegative initial condition. All solutions that begin with that starting data will therefore continue to be advantageous for any $t \geq 0$.*

Proof. Suppose $\bar{t} = \sup\{t \geq 0 : \mathbb{S}(t) \geq 0, \mathbb{P}(t) \geq 0, \mathbb{I}(t) \geq 0, \mathbb{T}(t) \geq 0, \mathbb{R}(t) \geq 0\}$, Clearly $\bar{t} \geq 0$. The first equation of the system leads to

$$\frac{d\mathbb{S}(t)}{dt} = b + c_1\mathbb{V} - \frac{k\mathbb{S}\mathbb{I}}{\mathbb{M}} - \mu_0\mathbb{S} - c_2\mathbb{S}, \tag{5}$$

from (5), we have

$$\frac{d\mathbb{S}(t)}{dt} + (\frac{k\mathbb{I}}{\mathbb{M}} + c_2 + \mu_0)\mathbb{S} = b + c_1\mathbb{V}, \tag{6}$$

now, put $b + c_1\mathbb{V} = b_1$ in (6), implies that

$$\frac{d\mathbb{S}(t)}{dt} = (\frac{k\mathbb{I}}{\mathbb{M}} + c_2 + \mu_0)\mathbb{S} = b_1. \tag{7}$$

take left hand of (7), as $\frac{k\mathbb{I}}{\mathbb{M}} + c_2 + \mu_0\mathbb{S} = g(t)$, so we have

$$\frac{d\mathbb{S}(t)}{dt} + g(t)\mathbb{S} = b_1,$$

By integrating factor, $I.F = e^{\int_0^t g(t)dt} = e^{\int_0^t g(t)\,dt}$,

$$\frac{d}{dt}\mathbb{S}(t)e^{\int_0^t g(t)}\,dt = b_1 e^{\int_0^t g(t)}\,dt,$$

integrating from $t = \bar{t}$ to $t = 0$, and multiply $e^{-\int_0^{\bar{t}} f(t)\,dt}$, we get

$$\mathbb{S}(\bar{t})e^{-\int_0^{\bar{t}} f(t)\,dt} = S(0)e^{-\int_0^{\bar{t}} f(t)\,dt} + b_1 e^{-\int_0^{\bar{t}} f(t)\,dt} \int_0^{\bar{t}} \left| e^{\int_0^y g(t)\,dt} \right| dy.$$

Since $\mathbb{S}(0) \geq 0$, the sum of the positive terms is positive, hence $\mathbb{S}(t)$ is positive. Similarly $\mathbb{V}(t)$, $\mathbb{E}(t)$, $\mathbb{I}(t)$, $\mathbb{T}(t)$, and $\mathbb{R}(t)$ for any set of nonnegative initial conditions used in $\mathcal{R}_+^6$ can be shown to hold for any $t \geq 0$. Moreover, the conclusion remains $x = 0$ for all $t \geq 0$ if $x_0 = 0$. $\mathcal{R}_+^6$ is therefore a positively invariant region. Which follow the conclusion.

Theorem 4. *The theorems (3.2) and (3.3) provide bounded solutions to the systems (1).*

Proof. The system (1) has positive solution using initial condition, $\mathbb{S}(0) \geq 0, \mathbb{V}(0) \geq 0, \mathbb{E}(0) \geq 0, \mathbb{I}(0) \geq 0, \mathbb{T}(0) \geq 0, \mathbb{R}(0) \geq 0$. To prove the bondness of the solution, we used the total population $\mathbb{M}(t)$ as,

$$\mathbb{M}(t) = \mathbb{S}(t) + \mathbb{V}(t) + \mathbb{E}(t), +\mathbb{I}(t) + \mathbb{T}(t) + \mathbb{R}(t)$$

Differentiating $\mathbb{M}(t)$ with respect to t and adding the six equation from system (1), we obtained that

$$\frac{d\mathbb{M}(t)}{dt} = b - \mu_0\mathbb{M}(t) - d_1\mathbb{I}(t) - d_2\mathbb{T}(t).$$

This implies that $\frac{d\mathbb{M}(t)}{dt} \leq b - \mu_0\mathbb{M}(t)$. By integrating, we get

$$\left|\ln\left(\frac{b - \mu_0\mathbb{M}(t)}{b - \mu_0\mathbb{M}(0)}\right)\right| \geq -\mu_0 t,$$

Simplify,

$$\mathbb{M}(t) \leq \frac{b}{\mu_0} + (\mathbb{M}(0) - \frac{b}{\mu_0})e^{-\mu_0 t}.$$

If we take $t \implies \infty$, then the factor $e^{-\mu_0 t} = 0$, So $\mathbb{M}(t) \leq \frac{b}{\mu_0}$. Hence all solution of the model (1) are bounded in the region ϕ.

$$\begin{aligned}\phi = \Big\{ (\mathbb{S}(t), \mathbb{V}(t), \mathbb{E}(t), \mathbb{I}(t), \mathbb{T}(t), \mathbb{R}(t)) \in \mathcal{R}_+^6 \,\Big|\, \\ \mathbb{S}(t) + \mathbb{V}(t) + \mathbb{E}(t) + \mathbb{I}(t) + \mathbb{T}(t) + \mathbb{R}(t) \leq \frac{b}{\mu_0}, \\ \mathbb{S}(t), \mathbb{V}(t), \mathbb{E}(t), \mathbb{I}(t), \mathbb{T}(t), \mathbb{R}(t) \geq 0 \Big\}\end{aligned}$$

As $\mathbb{M}(t) \leq \frac{b}{\mu_0}$, when time t approaches to infinity. Consequently, ϕ is a positively invariant closed set.

Thus, the proposed measle model (1) is well-posed and biologically meaningful since all of its solutions are positive and bounded.

Disease Free Equilibrium Points: In this section, we find the measle free equilibrium points for the system (1). The $\mathbb{SVEITR}$ model (1) has a unique measles free equilibrium point that is given as,

$$\begin{aligned}\mathcal{X}^0 &= \left(\mathbb{S}^0, \mathbb{V}^0\mathbb{E}^0, \mathbb{I}^0, \mathbb{T}^0, \mathbb{R}^0\right) \\ &= \left(\mathbb{S}^0, \mathbb{V}^0, 0, 0, 0, 0\right) \\ &= \left(\frac{b(c_1 + \mu_0)}{(c_2 + \mu_0)(c_1 + \mu_0) - c_1c_2}, \frac{bc_2}{(c_2 + \mu_0)(c_1 + \mu_0) - c_1c_2}, 0, 0, 0, 0\right).\end{aligned}$$

Endemic equilibrium:
The unique endemic equilibrium point $\mathcal{F}^*$ for the model (1) is also computed as in region ϕ, where

$$\mathbb{S}^*(t) = \frac{b(c_1+\mu_0)\mathbb{M}^*}{(k\mathbb{I}^* - (c_2+\mu_0)\mathbb{M}^*)(c_1+\mu_0) - c_1c_2\mathbb{M}^*},$$
$$\mathbb{V}^*(t) = \frac{c_2b(c_1+\mu_0)\mathbb{M}^*}{(c_1+\mu_0)[(k\mathbb{I}^* - (c_2+\mu_0)\mathbb{M}^*)(c_1+\mu_0) - c_1c_2\mathbb{M}^*]},$$
$$\mathbb{E}^*(t) = \frac{kb(c_1+\mu_0)\mathbb{I}^*}{(\alpha+r_1+\mu_0)[(k\mathbb{I}^* - (c_2+\mu_0)\mathbb{M}^*)(c_1+\mu_0) - c_1c_2\mathbb{M}^*]\mathbb{M}^*},$$
$$\mathbb{I}^*(t) = \frac{((c_2+\mu_0)(c_1+\mu_0)+c_1c_2)\mathbb{M}^*}{k(c_1+\mu_0} + \frac{\alpha kb}{k(c_2+d_1+\mu_0)(\alpha+r_1+\mu_0)\mathbb{M}^*},$$
$$\mathbb{T}^*(t) = \frac{\theta\mathbb{I}^*}{(r_2+d_2+\mu_0)},$$
$$\mathbb{R}^*(t) = \frac{r_2\theta\mathbb{I}^*}{\mu_0(r_2+d_2+\mu_0)} + \frac{r_1kb(c_1+\mu_0)\mathbb{I}^*}{(\alpha+r_1+\mu_0)[(k\mathbb{I}^* - (c_2+\mu_0)\mathbb{M}^*)(c_1+\mu_0) - c_1c_2\mathbb{M}^*]\mathbb{M}^*}.$$

4. Expression for $\mathcal{R}_0$

The basic reproduction number $\mathcal{R}_0$ is determined by analyzing the next-generation procedure in this section. The Basic Reproduction number $\mathbb{R}_0$ is a quantity used in epidemiology to describe how illness spreads and is controlled. We can determine the extent of the disease in the population and the best ways to protect community members from this deadly virus using $\mathbb{R}_0$. The following $\mathcal{R}_0$ is found using the next generation method, let $\Phi = (\mathcal{F}, \mathcal{E})$, then form system (1), we have

$$\frac{d\Phi}{dt} = \mathcal{F}(x) - \mathcal{E}(x)$$

Here we have

$$\mathcal{F}(x) = \begin{pmatrix} \frac{k\mathbb{S}\mathbb{I}}{\mathbb{M}} \\ 0 \\ 0 \end{pmatrix}, \mathcal{E}(x) = \begin{pmatrix} (\alpha+r_1+\mu_0)\mathbb{E} \\ (\theta+d_1+\mu_0)\mathbb{I} - \alpha\mathbb{E} \\ (r_2+d_2+\mu_0)\mathbb{T} - \theta\mathbb{I} \end{pmatrix}$$

When $\mathcal{F}$ and $\mathcal{E}$ are in disease-free equilibrium, their Jacobian at $\mathcal{X}^0$ is calculated,

$$\mathcal{F}(x) = \begin{pmatrix} 0 & \frac{k\mathbb{S}^0}{\mathbb{M}^0} & 0 \\ 0 & 0 & 0 \\ 0 & 0 & 0 \end{pmatrix}, \mathcal{E}(x) = \begin{pmatrix} (\alpha+r_1+\mu_0) & 0 & 0 \\ \alpha & (\theta+d_1+\mu_0) & 0 \\ 0 & \theta & (r_2+d_2+\mu_0) \end{pmatrix}$$

The basic reproduction number $\mathbb{R}_0$, is calculated as,

$$\mathbb{R}_0 = \rho(FV^-1)(\mathcal{X}^0) = \frac{k\alpha(c_1+\mu_0)}{(\alpha+r_1+\mu_0)(\theta+d_1+\mu_0)(c_1+c_2+\mu_0)}$$

Here, we arrive to the following conclusion based on the basic reproduction number $\mathbb{R}_0$.

5. Stability Analysis of DFE and EEP of model (1)

Here in this part of our work consisted of the stability analysis of the system (1). Furthermore, this section is divided into two subsections: local stability of the model and global stability of the model.

5.1. Local stability of disease free equilibrium (DFE)

In this section, we study the local stability of the measles model (1) in the next theorem by using the Jacobian matrix.

Theorem 5. *If $R_0 \leq 1$, the DFE of the system (1) about an equilibrium point F^0 is locally asymptotically stable (LAS); if $R_0 \geq 1$, it is unstable.*

Proof. The Jacobian Matrix at $\mathbb{J}^0$ is given below

$$\mathbb{J}(F^0) = \begin{bmatrix} -(c_2+\mu_0) & c_1 & 0 & \frac{-k\mu_0}{(c_2+\mu_0)(c_1+\mu_0)-c_1c_2} & 0 & 0 \\ c_2 & -(c_1+\mu_0) & 0 & 0 & 0 & 0 \\ 0 & 0 & -(\alpha+r_1+\mu_0) & \frac{k\mu_0}{(c_2+\mu_0)(c_1+\mu_0)-c_1c_2} & 0 & 0 \\ 0 & 0 & \alpha & -(\theta+d_1+\mu_0) & 0 & 0 \\ 0 & 0 & 0 & \theta & -(r_2+d_2+\mu_0) & 0 \\ 0 & 0 & r_1 & 0 & r_2 & -\mu_0 \end{bmatrix}.$$

The local stability criteria of Meals-free equilibrium are ascertained by analyzing the eigenvalues of the Jacobian matrix of the system (1) from columns C_6 and C_5, we determine two eigenvalues for direct expansion,and the required eigenvalue is given as:

$$\begin{aligned} \lambda_1 &= -\mu_0, \\ \lambda_2 &= -(r_2+d_2+\mu_0), \end{aligned} \tag{8}$$

and the Jacobian matrix is reduced to $4X4$ matrix as,

$$\mathbb{J}(F^0) = \begin{bmatrix} -(c_2+\mu_0) & c_1 & 0 & \frac{-k\mu_0}{(c_2+\mu_0)(c_1+\mu_0)-c_1c_2} \\ c_2 & -(c_1+\mu_0) & 0 & 0 \\ 0 & 0 & -(\alpha+r_1+\mu_0) & \frac{k\mu_0}{(c_2+\mu_0)(c_1+\mu_0)-c_1c_2} \\ 0 & 0 & \alpha & -(\theta+d_1+\mu_0) \end{bmatrix}.$$

A characteristic equation of this Jacobian matrix is given by:

$$\lambda^4 + a_1\lambda^3 + a_2\lambda^2 + a_3\lambda + a_4 = 0. \tag{9}$$

Here

$$\begin{aligned}
a_1 &= c_2 + c_1 + \alpha + r_1 + \theta + d_1 + 4\mu_0,\\
a_2 &= \frac{\mu_0(c_2 + c_1 + \mu_0)}{(\alpha + r_1 + \mu_0)(\theta + d_1 + \mu_0)} + \frac{(c_2 + c_1 + 2\mu_0)(\alpha + r_1 + \theta + d_1 + 2\mu_0)}{(\alpha + r_1 + \mu_0)(\theta + d_1 + \mu_0)} + (1 - R_0),\\
a_3 &= \frac{\mu_0(\alpha + r_1 + d_1 + 2\mu_0)(c_2 + c_1 + \mu_0)}{(c_2 + c_1 + 2\mu_0)(\alpha + r_1 + \mu_0)(\theta + d_1 + \mu_0)} + (1 - R_0),\\
a_4 &= \mu_0(c_2 + c_1 + \mu_0)(\alpha + r_1 + \mu_0)(\theta + d_1 + \mu_0)(1 - R_0).
\end{aligned} \tag{10}$$

Using the Routh-Hurwitz condition, $a_1a_2a_3 > a_3^2 + a_1^2a_4$. Hence our conclusion is gained as $\lambda_1 = -\mu_0 < 0$ and $\lambda_2 = -(r_2 + d_2 + \mu_0) < 0$. Also the condition $a_1a_2a_3 > a_3^2 + a_1^2a_4$ is hold from (9).

5.2. Global stability of disease free equilibrium (DFE)

Global stability of the model (1) is investigated by the following theorem.

Theorem 6. *If $k_5 \leq c_2$ and $R_0 \leq 1$, the DFE of the system (1) about an equilibrium point F^0 is globally asymptotically stable (GAS); if $R_0 \geq 1$, it is unstable.*

Proof. We define Lyapunov function as

$$\mathbb{U}(t) = \mathbb{A}_1\mathbb{E} + \mathbb{A}_2\mathbb{I} + \mathbb{A}_3\mathbb{T},$$

Take derivative with respect to t, we have

$$\dot{\mathbb{U}}(t) = \mathbb{A}_1\dot{\mathbb{E}} + \mathbb{A}_2\dot{\mathbb{I}} + \mathbb{A}_3\dot{\mathbb{T}}.$$

Putting the values from system (1), we get

$$\dot{\mathbb{U}(t)} \leq \mathbb{A}_2k_3\left(\frac{\mathbb{A}_1k + \mathbb{A}_3\theta}{\mathbb{A}_2k_3} - 1\right)\mathbb{I} + (\mathbb{A}_2\alpha + \mathbb{A}_1k_2)\mathbb{E} - (\mathbb{A}_3k_4)\mathbb{T}. \tag{11}$$

Where

$$\begin{aligned}
\mathbb{A}_1 &= c_1\alpha,\\
\mathbb{A}_2 &= K_2k_5,\\
\mathbb{A}_3 &= \frac{k\alpha\mu_0}{\theta}.
\end{aligned}$$

From (11), we have

$$\dot{\mathbb{U}(t)} \leq \frac{kk_3\alpha\mu_0}{\theta}(\mathbb{R}_0 - 1)\,\mathbb{I} + k_2\alpha(k_5 - c_1)\mathbb{E} - \left(\frac{kk_4\alpha\mu_0}{\theta}\right)\mathbb{T}.$$

So, we have $\dot{\mathbb{U}(t)} \leq 0$, if $k_5 \leq c_1$ and $R_0 \leq 1$ which follow the conclusion.

5.3. Local stability of endemic equilibrium point (EEP) $\mathcal{F}^*$

Theorem 7. *If $R_0 \geq 1$, the DEE of the system (1) about an equilibrium point $\mathcal{F}^*$ is (LAS) locally asymptotically stable otherwise unstable.*

Proof. The Jacobian Matrix at $\mathbb{J}^*$ is given below

$$\mathbb{J}(F^*) = \begin{bmatrix} -(k_0 + \frac{k\mathbb{I}^*}{\mathbb{M}^*}) - c_2^* & c_1 & 0 & -\frac{k\mathbb{S}^*}{\mathbb{M}^*} & 0 & 0 \\ c_2 & -k_1 - c_2^* & 0 & 0 & 0 & 0 \\ \frac{k\mathbb{I}^*}{\mathbb{M}^*} & 0 & -k_2 - c_2^* & \frac{k\mathbb{S}^*}{\mathbb{M}^*} & 0 & 0 \\ 0 & 0 & \alpha & -k_3 - c_2^* & 0 & 0 \\ 0 & 0 & 0 & \theta & -k_4 & 0 \\ 0 & 0 & r_1 & 0 & r_2 & -\mu_0 \end{bmatrix},$$

Local stability criteria of measles-endemic equilibrium are ascertained by analyzing the eigenvalues of the Jacobian matrix of the system (1) from columns C_6 and C_5, we determine two eigenvalues for direct expansion,and the required eigenvalue is given as: $\lambda_1 = -\mu_0$, and $\lambda_2 = -k_4 = -(r_2 + d_2 + \mu_0)$. Furthermore, the Jacobian matrix is reduced to $4X4$ matrix.

$$\mathbb{J}(\mathcal{F}^*) = \begin{bmatrix} -(k_0 + \frac{k\mathbb{I}^*}{\mathbb{M}^*}) - c_2^* & c_1 & 0 & -\frac{k\mathbb{S}^*}{\mathbb{M}^*} \\ c_2 & -k_1 - c_2^* & 0 & 0 \\ \frac{k\mathbb{I}^*}{\mathbb{M}^*} & 0 & -k_2 - c_2^* & \frac{k\mathbb{S}^*}{\mathbb{M}^*} \\ 0 & 0 & \alpha & -k_3 - c_2^* \end{bmatrix}.$$

The characteristic equation of the above Jacobian matrix is given as:

$$c_2^* + b_1 c_2^* + b_2 c_2^* + b_3 c_2^* + b_4 = 0.$$

Here

$$\begin{aligned} b_1 &= k_0 + k_1 k_2 k_3 + \frac{k\mathbb{I}^*}{\mathbb{M}^*}, \\ b_2 &= k_0(k_1 + k_2 + k_3) + \frac{k\mathbb{I}^*}{\mathbb{M}^*}(k_1 + k_2 + k_3) + k_1(k_2 + k_3) + (k_2 k_3) - \frac{k\mathbb{S}^*}{\mathbb{M}^*} - c_1, \\ b_3 &= k_1 k_2 k_3 - \frac{k k_1 \alpha \mathbb{S}^*}{\mathbb{M}^*} + k_0(k_1(k_2 + k_3) + k_2 k_3 - \frac{k\alpha\mathbb{S}^*}{\mathbb{M}^*}) + \frac{k\mathbb{I}^*}{\mathbb{M}^*}(k_1(k_2 + k_3) + k_2 k_3 - \frac{k\alpha\mathbb{S}^*}{\mathbb{M}^*}) - c_1(k_2 + k_3), \\ b_4 &= k_0 k_1 k_2 k_3 - \frac{k k_0 k_1 \alpha \mathbb{S}^*}{\mathbb{M}^*} + \frac{k k_1 k_2 k_3 \alpha \mathbb{I}^*}{\mathbb{M}^*} - \frac{k^2 k_1 \alpha \mathbb{S}^* \mathbb{I}^*}{\mathbb{M}^* 2} - c_1 k_2 k_3 + \frac{k\alpha\mathbb{S}^* c_1}{\mathbb{M}^*}. \end{aligned} \tag{12}$$

The value of characteristic polynomial, will be negative, if it satisfied the Routh-Hurwitz Criteria that is $n = 4, b_1 > 0, b_3 > 0, b_4 > 0$, and $b_1 b_2 b_3 > b_3^2 + a_1^2 a_4$, so we can say that (EEP) of the model (1) will be local asymptotically stable for $\mathcal{R}_0 > 1$.

5.4. Backward bifurcation analysis for Local stability of endemic equilibrium (EE)

Theorem 8. *[28] and [29] If $\mathcal{R}_0 > 1$, the DEE of the system (1) about an equilibrium point $\mathcal{F}^*$ is (LAS) Locally asymptotically stable otherwise unstable and also satisfy the condition $k_1 < 1$.*

Proof. Let $\mathbb{S} = x_1, \mathbb{V} = x_2, \mathbb{E} = x_3, \mathbb{I} = x_4, \mathbb{T} = x_5, \frac{dx_1}{dt} = h_1, \frac{dx_2}{dt} = h_2, \frac{dx_3}{dt} = h_3, \frac{dx_4}{dt} = h_4, \frac{dx_5}{dt} = h_5$, so the system (1) for first five equations with $\frac{d\mathbf{x}}{dt} = \mathbb{H}$, where $\mathbb{H} = (h_1, h_2, h_3, h_4, h_5)^T$ can be written as:

$$
\begin{aligned}
h_1(x) &= b + c_1x_2 - \frac{kx_1x_4}{\mathbb{M}} - \mu_0x_1 - c_2x_1 = b + c_1x_2 - \frac{kx_1x_4}{\mathbb{M}} - (\mu_0 + c_2)x_1 = b + c_1x_2 - \frac{kx_1x_4}{\mathbb{M}} - k_0x_1,\\
h_2(x) &= c_2x_1 - c_1x_2 - \mu_0x_2 = c_2x_1 - (c_1 + \mu_0)x_2 = c_2x_1 - k_1x_2,\\
h_3(x) &= \frac{kx_1x_4}{\mathbb{M}} - \alpha x_3 - r_1x_3 - \mu_0x_3 = \frac{kx_1x_4}{\mathbb{M}} - (\alpha - r_1 - \mu_0)x_3 = \frac{kx_1x_4}{\mathbb{M}} - k_2x_3,\\
h_4(x) &= \alpha x_3 - \theta x_4 - (d_1 + \mu_0)x_4 = \alpha x_3 - (\theta - d_1 + \mu_0)x_4 = \alpha x_3 - k_3x_4,\\
h_5(x) &= \theta x_4 - r_2x_5 - (d_2 + \mu_0)x_5 = \theta x_4 - (r_2 + d_2 + \mu_0)x_5 = \theta x_4 - k_4x_5.
\end{aligned}
\tag{13}
$$

To prove LAS of the system (1), We follow the center Manifold theory in [28], so we choose that $k = k^*$ as bifurcation parameter when $\mathcal{R}_0 = 1$ and assume that equilibrium point exist around the bifurcation point.

$$
k^* = k = \frac{(\alpha + r_1 + \mu_0)(\theta + d_1 + \mu_0)(c_2 + c_1 + \mu_0)}{\alpha(c_1 + \mu_0)} = \frac{k_2k_3(c_2 + c_1 + \mu_0)}{k_1\alpha}. \tag{14}
$$

So the Jacobian matrix can be calculated at disease-free equilibrium point $\mathcal{F}^0$ with k^* as

$$
\mathbb{J}(F^0, k^*) = \begin{bmatrix}
-(c_2 + \mu_0) & c_1 & 0 & \frac{-k^*\mu_0}{(c_2+\mu_0)(c_1+\mu_0)-c_1c_2} & 0\\
c_2 & -(c_1 + \mu_0) & 0 & 0 & 0\\
0 & 0 & -(\alpha + r_1 + \mu_0) & \frac{k^*\mu_0}{(c_2+\mu_0)(c_1+\mu_0)-c_1c_2} & 0\\
0 & 0 & \alpha & -(\theta + d_1 + \mu_0) & 0\\
0 & 0 & 0 & \theta & -(r_2 + d_2 + \mu_0)
\end{bmatrix}.
$$

Since the Jacobian matrix having a simple eigenvalue at k^*.So it can be seen that the left and right eigenvectors that is denoted by $\mathbb{W} = (w_1, w_2, w_3, w_4, w_5)$ and $\mathbb{V} = (v_1, v_2, v_3, v_4, v_5)$ respectively and calculated as;

$$
\begin{aligned}
w_1 &= (\frac{c_1+\mu_0}{c_2})w_2 > 0,\\
w_2 &> 0,\\
w_3 &= (\frac{\theta+eta_1+\mu_0}{\alpha})w_4 > 0,\\
w_4 &> 0,\\
w_5 &= (\frac{\theta}{r_2+d_2+\mu_0})w_4 > 0,
\end{aligned}
$$

and

$$
\begin{aligned}
v_1 &= (\frac{k_2k_3(c_2+\mu_0)(c_2+c_1+\mu_0)-k^*\alpha(c_1+\mu_0)}{k_2k^*(c_1+\mu_0)})v_4,\\
&= (\frac{k_0k_2k_3(c_2+c_1+\mu_0)-k_1k^*\alpha}{k_1k_2k^*})v_4,\\
v_2 &> 0,\\
v_3 &= (\frac{\alpha}{k_2})v_4,\\
v_4 &> 0,\\
v_5 &= 0.
\end{aligned}
$$

Evaluation of a:
By using,

$$\frac{\partial^2 g_1}{\partial x_1\partial x_4} = -\frac{k\mu_0}{b}, \frac{\partial^2 g_3}{\partial x_3\partial x_4} = \frac{k\mu_0}{b},$$

We calculate a from

$$\mathbf{a} = 2v_1w_1w_4\frac{\partial^2 g_1}{\partial x_1\partial x_4} + 2v_3w_1w_4\frac{\partial^2 g_3}{\partial x_3\partial x_4},$$

After simplification, we have

$$\mathbf{a} = 2\frac{k_1}{c_2}\frac{k\mu_0}{b}w_2w_4[(\frac{\alpha}{k_2}) + (\frac{k_0k^*\alpha - k_0k_2k_3(c_2+c_1+\mu_0)}{k_1k_2k^*})]v_4,$$

Since, we seen that all the terms in expression of **a** is positive except $k_0k^*\alpha - k_0k_2k_3(c_2+c_1+\mu_0)$, So $\mathbf{a} > 0$, iff $k_0k^*\alpha - k_0k_2k_3(c_2+c_1+\mu_0) > 0$, or simplify as $k_1 < 1$.
Evaluation of b:

$$\frac{\partial^2 g_1}{\partial x_4\partial k^*} = \frac{\partial^2 g_1}{\partial k^*\partial x_4} = -\frac{c_1+\mu_0}{(c_2+\mu_0)(c_2+c_1+\mu_0)} = -\frac{k_1}{k_0(c_2+c_1+\mu_0)}.$$

As;

$$\mathbf{b} = v_1w_4\frac{\partial^2 g_1}{\partial x_4\partial k^*} + v_3w_4\frac{\partial^2 g_3}{\partial x_4\partial k^*},$$

putting the values and simplify, we have

$$\mathbf{b} = w_4 \frac{k_1}{k_0(c_2+c_1+\mu_0)}[(\frac{\alpha}{k_2}) + (\frac{k_0k^*\alpha - k_0k_2k_3(c_2+c_1+\mu_0)}{k_1k_2k^*})]v_4,$$

Since as we seen that all the terms in expression of $\mathbf{b}$ is positive except $k_0k^*\alpha - k_0k_2k_3(c_2+c_1+\mu_0)$, So $\mathbf{b} > 0$, iff $k_0k^*\alpha - k_0k_2k_3(c_2+c_1+\mu_0) > 0$, or simplify as $k_1 < 1$.

According to Center Monifold Theory [28] and [29], the system (1) is locally asymptotically stable (LAS) around the bifurcation point at the endemic equilibrium point, as $\mathbf{a} > 0$ and $\mathbf{b} > 0$ for $k < 1$. As a result, when $R_0 = 1$, system (1) enters backward bifurcation mode. Because the endemic equilibrium point is LAS, illness will persist in the population for an extended period.

5.5. Global stability of endemic equilibrium (EE)

Theorem 9. *If $\mathcal{R}_0 \geq 1$, the DEE of the system (1) about an equilibrium point $\mathcal{F}^*$ is (GAS) globally asymptotically stable otherwise unstable.*

Proof. Consider a Lyapunov function $\mathbb{U}_1(t) : \mathbb{Q} \implies \mathbb{R}$ defined by,

$$\mathbb{U}_1(t) = \left(\mathbb{S} - \mathbb{S}^* - \mathbb{S}^*\frac{\ln \mathbb{S}(t)}{\mathbb{S}^*}\right) + \left(\mathbb{V} - \mathbb{V}^* - \mathbb{V}^*\frac{\ln \mathbb{V}(t)}{\mathbb{V}^*}\right) + \left(\mathbb{E} - \mathbb{E}^* - \mathbb{E}^*\frac{\ln \mathbb{E}(t)}{\mathbb{E}^*}\right) + \left(\mathbb{I} - \mathbb{I}^* - \mathbb{I}^*\frac{\ln \mathbb{I}(t)}{\mathbb{I}^*}\right) + \mathbb{T}^*\left(\frac{k_2+1}{\theta\mathbb{I}^*}\right)\left(\mathbb{T} - \mathbb{T}^* - \mathbb{T}^*\frac{\ln \mathbb{T}(t)}{\mathbb{T}^*}\right),$$

We want to show the global stability at point $\mathcal{F}^*$.
Differentiate of $\mathbb{U}_1(t)$ with respect to t, gives us

$$\mathbb{U}_1'(t) = \left(1 - \frac{\mathbb{S}^*}{\mathbb{S}}\right)\mathbb{S}' + \left(1 - \frac{\mathbb{V}^*}{\mathbb{V}}\right)\mathbb{V}' + \left(1 - \frac{\mathbb{E}^*}{\mathbb{E}}\right)\mathbb{E}' + \left(1 - \frac{\mathbb{I}^*}{\mathbb{I}}\right)\mathbb{I}' + \mathbb{T}^*\left(\frac{k_2+1}{\theta\mathbb{I}^*}\right)\left(1 - \frac{\mathbb{T}^*}{\mathbb{T}}\right)\mathbb{T}', \tag{15}$$

let consider first two terms from (15), we have

$$\begin{aligned}\left(1 - \frac{\mathbb{S}^*}{\mathbb{S}}\right)\mathbb{S}' + \left(1 - \frac{\mathbb{V}^*}{\mathbb{V}}\right)\mathbb{V}' &= \left(1 - \frac{\mathbb{S}^*}{\mathbb{S}}\right)\left(b + c_1\mathbb{V} - \frac{k\mathbb{I}\mathbb{S}}{N} - c_2\mathbb{S} - \mu_0\mathbb{S}\right) + \left(1 - \frac{\mathbb{V}^*}{\mathbb{V}}\right)(c_2\mathbb{S} - c_1\mathbb{V} - \mu_0\mathbb{V}),\\ &= \left(1 - \frac{\mathbb{S}^*}{\mathbb{S}}\right)\left(b + c_1\mathbb{V} - \frac{k\mathbb{I}\mathbb{S}}{N} - c_2\mathbb{S} - \mu_0\mathbb{S} - c_1\mathbb{V}^* + \frac{k\mathbb{I}^*\mathbb{S}^{**}}{N} + c_2\mathbb{S}^* - \mu_0\mathbb{S}^*\right),\end{aligned}$$

after simplification,

$$\begin{aligned}\left(1 - \frac{\mathbb{S}^*}{\mathbb{S}}\right)\mathbb{S}' + \left(1 - \frac{\mathbb{V}^*}{\mathbb{V}}\right)\mathbb{V}' &= \frac{k\mathbb{I}^*\mathbb{S}^{**}}{N}\left(1 - \frac{\mathbb{S}^*}{S} - \frac{\mathbb{I}\mathbb{S}\mathbb{M}^*}{\mathbb{I}^*\mathbb{S}^*\mathbb{M}}\right) + c_2\mathbb{S}^*\left(2 - \frac{\mathbb{S}^*}{\mathbb{S}} - \frac{\mathbb{S}\mathbb{V}^*}{\mathbb{S}^*\mathbb{V}}\right) + \mu_0\mathbb{S}^*\left(2 - \frac{\mathbb{S}}{\mathbb{S}^*} - \frac{\mathbb{S}^*}{\mathbb{S}}\right)\\ &\quad + c_1\mathbb{V}^*\left(\frac{\mathbb{S}}{\mathbb{S}^*} - \frac{\mathbb{S}^*\mathbb{V}}{\mathbb{S}\mathbb{V}^*}\right) + \frac{k\mathbb{I}\mathbb{S}^*}{\mathbb{M}} - \mu_0\mathbb{V} + \mu_0\mathbb{V}^*,\end{aligned} \tag{16}$$

first we solve; $-\mu_0\mathbb{V}+\mu_0\mathbb{V}^*$ consider,

$$\mu_0\mathbb{V}^*-\mu_0\mathbb{V}=\mu_0\mathbb{V}^*\left(1-\frac{\mathbb{V}}{\mathbb{V}^*}\right), \tag{17}$$

we know that,

$$\mu_0\mathbb{V}^*=c_2\mathbb{S}^*-c_1\mathbb{V}^*,$$

So (17) becomes,

$$\begin{aligned}\mu_0\mathbb{V}^*-\mu_0\mathbb{V}&=\left(c_2\mathbb{S}^*-c_1\mathbb{V}^*\right)\left(1-\frac{\mathbb{V}}{\mathbb{V}^*}\right),\\&=c_2\mathbb{S}^*-c_1\mathbb{V}^*+c_2\mathbb{S}^*\frac{\mathbb{V}^*}{\mathbb{V}}+c_1\mathbb{V},\\&=c_2\mathbb{S}^*\left(1-\frac{\mathbb{V}^*}{\mathbb{V}}\right)+c_1\mathbb{V}^*\left(-1+\frac{\mathbb{V}}{\mathbb{V}^*}\right),\end{aligned}$$

Putting these values in (16), so we get

$$\begin{aligned}\left(1-\frac{\mathbb{S}^*}{\mathbb{S}}\right)\mathbb{S}'+\left(1-\frac{\mathbb{V}^*}{\mathbb{V}}\right)\mathbb{V}'&=\frac{k\mathbb{I}^*\mathbb{S}^*}{\mathbb{M}^*}\left(1-\frac{\mathbb{S}^*}{\mathbb{S}}-\frac{\mathbb{I}\mathbb{S}\mathbb{M}^*}{\mathbb{I}^*\mathbb{S}^*\mathbb{M}}\right)\\&\quad+c_2\mathbb{S}^*\left(2-\frac{\mathbb{S}^*}{\mathbb{S}}-\frac{\mathbb{S}\mathbb{V}^*}{\mathbb{S}^*\mathbb{V}}\right)+\mu_0\mathbb{S}^*\left(2-\frac{\mathbb{S}}{\mathbb{S}^*}-\frac{\mathbb{S}^*}{\mathbb{S}}\right)\\&\quad+c_1\mathbb{V}^*\left(\frac{\mathbb{S}}{\mathbb{S}^*}-\frac{\mathbb{S}^*\mathbb{V}}{\mathbb{S}\mathbb{V}^*}\right)+c_2\mathbb{S}^*\left(1-\frac{\mathbb{V}^*}{\mathbb{V}}\right)+c_1\mathbb{V}^*\left(-1+\frac{\mathbb{V}}{\mathbb{V}^*}\right)+\frac{k\mathbb{I}\mathbb{S}^*}{\mathbb{M}}\\&=\frac{k\mathbb{I}^*\mathbb{S}^*}{\mathbb{M}^*}\left(1-\frac{\mathbb{S}^*}{\mathbb{S}}-\frac{\mathbb{I}\mathbb{S}\mathbb{M}^*}{\mathbb{I}^*\mathbb{S}^*\mathbb{M}}\right)\\&\quad+c_2\mathbb{S}^*\left(3-\frac{\mathbb{S}^*}{\mathbb{S}}-\frac{\mathbb{V}^*}{\mathbb{V}}-\frac{\mathbb{S}\mathbb{V}^*}{\mathbb{S}^*\mathbb{V}}\right)+\mu_0\mathbb{S}^*\left(2-\frac{\mathbb{S}}{\mathbb{S}^*}-\frac{\mathbb{S}^*}{\mathbb{S}}\right)\\&\quad+c_1\mathbb{V}^*\left(1-\frac{\mathbb{S}^*\mathbb{V}}{\mathbb{S}\mathbb{V}^*}-\left(1-\frac{\mathbb{V}^*}{\mathbb{V}}\right)-\left(1-\frac{\mathbb{S}^*}{\mathbb{S}}\right)\right)+\frac{k\mathbb{I}\mathbb{S}^*}{\mathbb{M}}.\end{aligned} \tag{18}$$

Next we consider,

$$\begin{aligned}\left(1-\frac{\mathbb{E}^*}{\mathbb{E}}\right)\mathbb{E}'+\left(1-\frac{\mathbb{I}^*}{\mathbb{I}}\right)\mathbb{I}'&=\left(1-\frac{\mathbb{E}^*}{\mathbb{E}}\right)\left(\frac{k\mathbb{S}\mathbb{I}}{\mathbb{M}}-k_2\mathbb{E}\right)+\left(1-\frac{\mathbb{I}^*}{\mathbb{I}}\right)\left(\alpha\mathbb{E}-k_3\mathbb{I}\right),\\&=-\frac{k\mathbb{I}\mathbb{S}\mathbb{E}^*}{\mathbb{M}\mathbb{E}}+\frac{k\mathbb{I}\mathbb{S}}{\mathbb{M}}-k_2\mathbb{E}+k_2\mathbb{E}^*+\alpha\mathbb{E}-k_3\mathbb{I}-\alpha\mathbb{E}\frac{I^*}{I}+k_3\mathbb{I}^*.\end{aligned}$$

Now putting the value of $k_2=\alpha+r_1+\mu_0$ in above equation, so we get,

$$\begin{aligned}\left(1-\frac{\mathbb{E}^*}{\mathbb{E}}\right)\mathbb{E}'+\left(1-\frac{\mathbb{I}^*}{\mathbb{I}}\right)\mathbb{I}'&=-\frac{k\mathbb{I}\mathbb{S}\mathbb{E}^*}{\mathbb{M}\mathbb{E}}+\frac{k\mathbb{I}\mathbb{S}}{\mathbb{M}}+\alpha\mathbb{E}-k_3\mathbb{I}-\alpha\mathbb{E}\frac{\mathbb{I}^*}{\mathbb{I}}+k_3\mathbb{I}^*-\left(\alpha+r_1+\mu_0\right)\mathbb{E}+\left(\alpha+r_1+\mu_0\right)\mathbb{E}^*\\&=-\frac{k\mathbb{I}\mathbb{S}\mathbb{E}^*}{\mathbb{M}\mathbb{E}}+\frac{k\mathbb{I}\mathbb{S}}{\mathbb{M}}+\alpha\mathbb{E}^*\left(1-\frac{\mathbb{E}}{\mathbb{E}^*}-\frac{\mathbb{E}\mathbb{I}^*}{\mathbb{E}^*\mathbb{I}}\left(1-\frac{\mathbb{I}}{\mathbb{I}^*}\right)\right)\\&\quad+\left(r_1+\mu_0\right)\mathbb{E}^*\left(1-\frac{\mathbb{E}}{\mathbb{E}^*}\right)+k_3\mathbb{I}^*\left(1-\frac{\mathbb{I}}{\mathbb{I}^*}\right)\end{aligned}$$

we know that $k_3\mathbb{I}^* = \alpha\mathbb{E}^*$, by putting in above equation, we get.

$$\begin{aligned}\left(1-\frac{\mathbb{E}^*}{\mathbb{E}}\right)\mathbb{E}' + \left(1-\frac{\mathbb{I}^*}{\mathbb{I}}\right)\mathbb{I}' &= -\frac{k\mathbb{I}\mathbb{S}\mathbb{E}^*}{\mathbb{M}\mathbb{E}} + \frac{k\mathbb{I}\mathbb{S}}{\mathbb{M}} + \alpha\mathbb{E}^*\left(1-\frac{\mathbb{E}}{\mathbb{E}^*} - \frac{\mathbb{E}\mathbb{I}^*}{\mathbb{E}^*\mathbb{I}}\left(1-\frac{\mathbb{I}}{\mathbb{I}^*}\right)\right)\\ &\quad + (r_1+\mu_0)\mathbb{E}^*\left(1-\frac{\mathbb{E}}{\mathbb{E}^*}\right) + \alpha\mathbb{E}^*\left(1-\frac{\mathbb{I}}{\mathbb{I}^*}\right),\\ &= -\frac{k\mathbb{I}\mathbb{S}\mathbb{E}^*}{\mathbb{M}\mathbb{E}} + \frac{k\mathbb{I}\mathbb{S}}{\mathbb{M}} + \alpha\mathbb{E}^*\left(2-\frac{\mathbb{E}}{\mathbb{E}^*} - \frac{\mathbb{I}}{\mathbb{I}^*} - \frac{\mathbb{E}\mathbb{I}^*}{\mathbb{E}^*\mathbb{I}}\left(1-\frac{\mathbb{I}}{\mathbb{I}^*}\right)\right)\\ &\quad + (r_1+\mu_0)\mathbb{E}^*\left(1-\frac{\mathbb{E}}{\mathbb{E}^*}\right).\end{aligned} \tag{19}$$

Adding equations (18) and (19), we get;

$$\begin{aligned}&\left(1-\frac{\mathbb{S}^*}{\mathbb{S}}\right)\mathbb{S}' + \left(1-\frac{\mathbb{V}^*}{\mathbb{V}}\right)\mathbb{V}' + \left(1-\frac{\mathbb{E}^*}{\mathbb{E}}\right)\mathbb{E}' + \left(1-\frac{\mathbb{I}^*}{\mathbb{I}}\right)\mathbb{I}' = \frac{k\mathbb{I}^*\mathbb{S}^*}{\mathbb{M}^*}\left(1-\frac{\mathbb{S}^*}{S} - \frac{\mathbb{I}\mathbb{S}\mathbb{M}^*\mathbb{E}^*}{\mathbb{I}^*\mathbb{S}^*\mathbb{M}\mathbb{E}}\right)\\ &+ c_2\mathbb{S}^*\left(3-\frac{\mathbb{S}^*}{\mathbb{S}} - \frac{\mathbb{V}^*}{\mathbb{V}} - \frac{\mathbb{S}\mathbb{V}^*}{\mathbb{S}^*\mathbb{V}}\right) + \mu_0\mathbb{S}^*\left(2-\frac{\mathbb{S}}{\mathbb{S}^*} - \frac{\mathbb{S}^*}{\mathbb{S}}\right) + c_1\mathbb{V}^*\left(1-\frac{\mathbb{S}^*\mathbb{V}}{\mathbb{S}\mathbb{V}^*} - \left(1-\frac{\mathbb{V}^*}{\mathbb{V}}\right) - \left(1-\frac{\mathbb{S}^*}{\mathbb{S}}\right)\right)\\ &+ \alpha\mathbb{E}^*(2-\frac{\mathbb{E}}{\mathbb{E}^*} - \frac{\mathbb{I}}{\mathbb{I}^*} - \frac{\mathbb{E}\mathbb{I}^*}{\mathbb{E}^*\mathbb{I}}\left(1-\frac{\mathbb{I}}{\mathbb{I}^*}\right) + (r_1+\mu_0)\mathbb{E}^*\left(1-\frac{\mathbb{E}^*}{\mathbb{E}}\right) + \frac{k\mathbb{I}\mathbb{S}^*}{\mathbb{M}},\end{aligned} \tag{20}$$

last two terms of

$$(r_1+\mu_0)(1-\frac{\mathbb{E}^*}{\mathbb{E}})\mathbb{E}^* + \frac{k\mathbb{I}\mathbb{S}^*}{\mathbb{M}} = (r_1+\mu_0)\mathbb{E}^* - (r_1+\mu_0)\mathbb{E}^* + \frac{k\mathbb{I}\mathbb{S}^*}{\mathbb{M}} \tag{21}$$

Since; $k_2\mathbb{E}^* = \frac{k\mathbb{I}^*\mathbb{S}^*}{\mathbb{M}^*}$ or $k = \frac{k_2\mathbb{E}^*\mathbb{M}^*}{\mathbb{S}^*\mathbb{I}^*}$, putting values in (21), so we get,

$$\begin{aligned}(r_1+\mu_0)\left(1-\frac{\mathbb{E}^*}{\mathbb{E}}\right)\mathbb{E}^* + \frac{k\mathbb{I}\mathbb{S}^*}{\mathbb{M}} &= (r_1+\mu_0)\mathbb{E}^* - (r_1+\mu_0)\mathbb{E} + \frac{k_2\mathbb{E}^*\mathbb{M}^*}{\mathbb{M}\mathbb{I}^*},\\ &= (r_1+\mu_0)\mathbb{E}^* - (r_1+\mu_0)\mathbb{E} + \frac{\mathbb{I}\mathbb{M}^*}{\mathbb{I}^*\mathbb{M}}(\alpha+r_1+\mu_0)\,\mathbb{E}^*,\\ &= (r_1+\mu_0)\mathbb{E}^* - (r_1+\mu_0)\mathbb{E} + (r_1+\mu_0)\mathbb{E}^*\left(\frac{\mathbb{I}\mathbb{M}^*}{\mathbb{I}^*\mathbb{M}}\right) + \alpha\mathbb{E}^*\left(\frac{\mathbb{I}\mathbb{M}^*}{\mathbb{I}^*\mathbb{M}}\right),\\ &= (r_1+\mu_0)\mathbb{E}^*\left(1-\frac{\mathbb{E}}{\mathbb{E}^*} + \frac{\mathbb{I}\mathbb{M}^*}{\mathbb{I}^*\mathbb{M}}\right) + \alpha\mathbb{E}^*\left(\frac{\mathbb{I}\mathbb{M}^*}{\mathbb{I}^*\mathbb{M}}\right),\\ &= (r_1+\mu_0)\mathbb{E}^*\left(1+1-\frac{\mathbb{E}}{\mathbb{E}^*} - 1 + \frac{\mathbb{I}\mathbb{M}^*}{\mathbb{I}^*\mathbb{M}} + \alpha\mathbb{E}^*\left(\frac{\mathbb{I}\mathbb{M}^*}{\mathbb{I}^*\mathbb{M}}\right)\right),\\ &= (r_1+\mu_0)\mathbb{E}^*\left(2-\frac{\mathbb{E}}{\mathbb{E}^*} - \left(1-\frac{\mathbb{I}\mathbb{M}^*}{\mathbb{I}^*\mathbb{M}}\right) + \alpha\mathbb{E}^*\left(\frac{\mathbb{I}\mathbb{M}^*}{\mathbb{I}^*\mathbb{M}}\right)\right).\end{aligned}$$

Putting this values in equation (20), we get;

$$\left(1-\frac{\mathbb{S}^*}{\mathbb{S}}\right)\mathbb{S}^{'}+\left(1-\frac{\mathbb{V}^*}{\mathbb{V}}\right)\mathbb{V}^{'}+\left(1-\frac{\mathbb{E}^*}{\mathbb{E}}\right)\mathbb{E}^{'}+\left(1-\frac{\mathbb{I}^*}{\mathbb{I}}\right)\mathbb{I}^{'}=\frac{k\mathbb{I}^*\mathbb{S}^*}{\mathbb{M}^*}\left(1-\frac{\mathbb{S}^*}{S}-\frac{\mathbb{I}\mathbb{S}\mathbb{M}^*\mathbb{E}^*}{\mathbb{I}^*\mathbb{S}^*\mathbb{M}\mathbb{E}}\right)$$
$$+c_2\mathbb{S}^*\left(3-\frac{\mathbb{S}^*}{\mathbb{S}}-\frac{\mathbb{V}^*}{\mathbb{V}}-\frac{\mathbb{S}\mathbb{V}^*}{\mathbb{S}^*\mathbb{V}}\right)+\mu_0\mathbb{S}^*\left(2-\frac{\mathbb{S}}{\mathbb{S}^*}-\frac{\mathbb{S}^*}{\mathbb{S}}\right)+c_1\mathbb{V}^*(1-\frac{\mathbb{S}^*\mathbb{V}}{\mathbb{S}\mathbb{V}^*}-(1-\frac{\mathbb{V}^*}{\mathbb{V}})-(1-\frac{\mathbb{S}^*}{\mathbb{S}}))$$
$$+\alpha\mathbb{E}^*\left(2-\frac{\mathbb{E}}{\mathbb{E}^*}-\frac{\mathbb{I}}{\mathbb{I}^*}+\frac{\mathbb{I}\mathbb{M}^*}{\mathbb{I}^*\mathbb{M}}-\frac{\mathbb{E}\mathbb{I}^*}{\mathbb{E}^*\mathbb{I}}\left(1-\frac{\mathbb{I}}{\mathbb{I}^*}\right)+(r_1+\mu_0)\mathbb{E}^*\left(2-\frac{\mathbb{E}^*}{\mathbb{E}}-\left(1-\frac{\mathbb{I}\mathbb{M}^*}{\mathbb{I}^*\mathbb{M}}\right)\right)\right). \tag{22}$$

Now, we consider last term from equation (15),

$$\mathbb{T}^*(\frac{k_1+1}{\theta\mathbb{I}^*})(1-\frac{\mathbb{T}^*}{\mathbb{T}})\mathbb{T}'=\mathbb{T}^*(\frac{k_1+1}{\theta\mathbb{I}^*})(1-\frac{\mathbb{T}^*}{\mathbb{T}})(\theta\mathbb{I}-k_4\mathbb{T})$$

Since $k_4\mathbb{T}^*=\theta\mathbb{I}^* \implies k_4=\frac{\theta\mathbb{I}^*}{\mathbb{T}^*}$

$$\begin{aligned}
\mathbb{T}^*\left(\frac{k_1+1}{\theta\mathbb{I}^*}\right)\left(1-\frac{\mathbb{T}^*}{\mathbb{T}}\right)\mathbb{T}' &= \mathbb{T}^*\left(\frac{k_1+1}{\theta\mathbb{I}^*}\right)\left(1-\frac{\mathbb{T}^*}{\mathbb{T}}\right)\left(\theta\mathbb{I}-\frac{\theta\mathbb{I}^{'}}{\mathbb{T}^*}\mathbb{T}\right),\\
&= \theta(\mathbb{T}^*\left(\frac{k_1+1}{\theta\mathbb{I}^*}\right)\left(1-\frac{\mathbb{T}^*}{\mathbb{T}}\right)\left(\mathbb{I}-\frac{\mathbb{I}^{'}}{\mathbb{T}^*}\mathbb{T}\right),\\
&= \mathbb{T}^*\left(\frac{k_1+1}{\mathbb{I}^*}\right)\left(1-\frac{\mathbb{T}^*}{\mathbb{T}}\right)\left(\mathbb{I}-\frac{\mathbb{I}^{'}}{\mathbb{T}^*}\mathbb{T}\right),\\
&= \frac{k_1\mathbb{T}^*+\mathbb{T}^*}{\mathbb{I}^*}\left(\mathbb{I}+\mathbb{I}^*-\frac{\mathbb{T}\mathbb{I}^*}{\mathbb{T}^*}-\frac{\mathbb{T}^*\mathbb{I}}{\mathbb{T}}\right),\\
&= \frac{k_1\mathbb{T}^*\mathbb{I}}{\mathbb{I}^*}+k_1\mathbb{T}^*-k_1\mathbb{T}-\frac{k_1\mathbb{T}^{*2}\mathbb{I}}{\mathbb{T}\mathbb{I}^*}+\frac{\mathbb{T}^*\mathbb{I}}{\mathbb{I}^*}+\mathbb{T}^*-\mathbb{T}-\frac{\mathbb{T}^{*2}\mathbb{I}}{\mathbb{T}\mathbb{I}^*},\\
&= \mathbb{T}^*\left(1-\frac{\mathbb{T}^*}{\mathbb{T}}-\frac{\mathbb{T}^*\mathbb{I}}{\mathbb{T}\mathbb{I}^*}+\frac{\mathbb{I}}{\mathbb{I}^*}\right)+k_1\mathbb{T}^*\left(1-\frac{\mathbb{T}^*}{\mathbb{T}}-\frac{\mathbb{T}^*\mathbb{I}}{\mathbb{T}\mathbb{I}^*}+\frac{\mathbb{I}}{\mathbb{I}^*}\right),\\
&= \mathbb{T}^*\left(1-\frac{\mathbb{T}^*}{\mathbb{T}}-\frac{\mathbb{T}^*\mathbb{I}}{\mathbb{T}\mathbb{I}^*}(1-\frac{\mathbb{T}}{\mathbb{T}^*})\right)+k_1\mathbb{T}^*\left(1-\frac{\mathbb{T}^*}{\mathbb{T}}-\frac{\mathbb{T}^*\mathbb{I}}{\mathbb{T}\mathbb{I}^*}\left(1-\frac{\mathbb{T}}{\mathbb{T}^*}\right)\right).
\end{aligned} \tag{23}$$

Adding equations (22) and (23), so finally we get;

$$\begin{aligned}
\mathbb{U}_1^{'}(t) &= \left(1-\frac{\mathbb{S}^*}{\mathbb{S}}\right)\mathbb{S}^{'}+\left(1-\frac{\mathbb{V}^*}{\mathbb{V}}\right)\mathbb{V}^{'}+\left(1-\frac{\mathbb{E}^*}{\mathbb{E}}\right)\mathbb{E}^{'}+\left(1-\frac{\mathbb{I}^*}{\mathbb{I}}\right)\mathbb{I}^{'}\\
&\quad+\mathbb{T}^*\left(\frac{k_1+1}{\theta\mathbb{I}^*}\right)\left(1-\frac{\mathbb{T}^*}{\mathbb{T}}\right)\mathbb{T}^{'}\\
&= \frac{k\mathbb{I}^*\mathbb{S}^*}{\mathbb{M}^*}\left(1-\frac{\mathbb{S}^*}{\mathbb{S}}-\frac{\mathbb{I}\mathbb{S}\mathbb{M}^*\mathbb{E}^*}{\mathbb{I}^*\mathbb{S}^*\mathbb{M}\mathbb{E}}\right)
\end{aligned}$$

$$
\begin{aligned}
&+ c_2\mathbb{S}^*\left(3 - \frac{\mathbb{S}^*}{\mathbb{S}} - \frac{\mathbb{V}^*}{\mathbb{V}} - \frac{\mathbb{S}\mathbb{V}^*}{\mathbb{S}^*\mathbb{V}}\right) + \mu_0\mathbb{S}^*\left(2 - \frac{\mathbb{S}}{\mathbb{S}^*} - \frac{\mathbb{S}^*}{\mathbb{S}}\right)\\
&+ c_1\mathbb{V}^*\left(1 - \frac{\mathbb{S}^*\mathbb{V}}{\mathbb{S}\mathbb{V}^*} - \left(1 - \frac{\mathbb{V}^*}{\mathbb{V}}\right) - \left(1 - \frac{\mathbb{S}^*}{\mathbb{S}}\right)\right)\\
&+ \alpha\mathbb{E}^*\left(2 - \frac{\mathbb{E}}{\mathbb{E}^*} - \frac{\mathbb{I}}{\mathbb{I}^*} + \frac{\mathbb{I}\mathbb{M}^*}{\mathbb{I}^*\mathbb{M}} - \frac{\mathbb{E}\mathbb{I}^*}{\mathbb{E}^*\mathbb{I}}\left(1 - \frac{\mathbb{I}}{\mathbb{I}^*}\right)\right)\\
&+ (r_1 + \mu_0)\mathbb{E}^*\left(2 - \frac{\mathbb{E}}{\mathbb{E}^*} - \left(1 - \frac{\mathbb{I}\mathbb{M}^*}{\mathbb{I}^*\mathbb{M}}\right)\right)\\
&+ \mathbb{T}^*\left(1 - \frac{\mathbb{T}^*}{\mathbb{T}} - \frac{\mathbb{T}^*\mathbb{I}}{\mathbb{T}\mathbb{I}^*}\left(1 - \frac{\mathbb{T}}{\mathbb{T}^*}\right)\right)\\
&+ k_1\mathbb{T}^*\left(1 - \frac{\mathbb{T}^*}{\mathbb{T}} - \frac{\mathbb{T}^*\mathbb{I}}{\mathbb{T}\mathbb{I}^*}\left(1 - \frac{\mathbb{T}}{\mathbb{T}^*}\right)\right). \qquad (24)
\end{aligned}
$$

The following inequality from equation (24) is true since the arithmetic mean is greater than the geometric mean: Hence, we conclude that $\mathbb{U}_1^{'}(t) \leq 0$, because the geometric mean is smaller than the arithmetic mean, and exercise the LaSalle's Invariance rule, we get that the measle model (1) is global asymptotically stable at EEP $\mathcal{F}^*$, when $\mathcal{R}_0 \geq 1$.

6. Sensitivity Analysis

This section presents the sensitivity analysis that account for all variables that significantly affect the basic reproduction number $\mathcal{R}_0$. Sensitivity analysis is recommended to determine the importance of the numerous factors affecting the occurrence and spread of disease. In addition to preventing the spread of diseases, obtaining $\mathcal{R}_0 < 1$ needs managing the system (**??**) variables. The sensitive index, which shows the ratio of modifications in an element to changes in a parameter, can be calculated using the formula. The sensitivity index for each parameter involved in the fundamental reproduction numbers $\mathcal{R}_0 < 1$ is shown in the next 1.

$$g[y] = \frac{X}{\mathcal{R}_0}\frac{\partial \mathcal{R}_0}{\partial X},$$

where X average factor of $\mathbb{R}_0$ is the formula used to calculate the The variables of infection constant k and infection rate of measles α are the primary variables that boost the basic reproduction number $\mathcal{R}_0$, while the death rate c_2 and vaccination rate c_1 is the main factor that decreases the basic reproduction number $\mathcal{R}_0$. These parameters are directly related to $\mathcal{R}_0$. This is evident from Table (1) and Fig. (1). Nonetheless, the variables that have a minor impact on the fundamental reproduction number to increase are c_1, while θ, d_1 and μ_0 are the factors which show decay in the infection flow. The next figure (2) describes the $\mathbb{R}_0$'s 3D dynamics.

Variables	Sensitivity Index
$g(k)$	1
$g(\alpha)$	0.6402
$g(\mu_0)$	0.0042
$g(r_1)$	-0.6139
$g(\theta)$	-0.8866
$g(d_1)$	-0.06795
$g(c_2)$	-0.5928
$g(c_1)$	0.5168

Table 1: The parameters and their description involved in sensitivity analysis of the model for R_0 (1).

7. Numerical Analysis

The deterministic system (1) is numerically simulated in this part using the non-standard finite difference technique (NSFD) [37, 38]. First, the model equations are expressed as follows: As an example, the first system equation (1),

$$\frac{d\mathbb{S}(t)}{dt} = b + c_1\mathbb{V} - \frac{k\mathbb{S}\mathbb{I}}{\mathbb{M}} - (c_2 + \mu_0)\mathbb{S}. \tag{25}$$

From the none-standard finite difference method, we decomposed as

$$\frac{\mathbb{S}_{j+1} - \mathbb{S}_j}{h} = b + c_1\mathbb{V}_j - \frac{k\mathbb{S}_j\mathbb{I}_j}{\mathbb{M}} - (c_2 + \mu_0)\mathbb{S}_j. \tag{26}$$

Further model equations (1) have been scaled down using the non-standard finite difference method, similar to (26).

$$\begin{aligned}
\mathbb{V}_{j+1} &= \mathbb{V}_j + h\bigg(c_2\mathbb{S}_j - c_1\mathbb{V}_j - \mu_0\mathbb{V}_j\bigg),\\
\mathbb{E}_{j+1} &= \mathbb{E}_j + h\bigg(\frac{k\mathbb{S}_j\mathbb{I}_j}{\mathbb{M}} - \alpha\mathbb{E}_j - r_1\mathbb{E}_j - \mu_0\mathbb{E}_j\bigg),\\
\mathbb{I}_{j+1} &= \mathbb{I}_j + h\bigg(\alpha\mathbb{E}_j - \theta)\mathbb{I}_j - (d_1 + \mu_0)\mathbb{I}_j\bigg),\\
\mathbb{T}_{j+1} &= \mathbb{T}_j + h\bigg(\theta\mathbb{I}_j - r_2\mathbb{T}_j - (d_2 + \mu_0)\mathbb{T}_j\bigg),\\
\mathbb{R}_{j+1} &= \mathbb{R}_j + h\bigg(r_2\mathbb{T}_j + r_1\mathbb{E}_j - \mu_0\mathbb{R}_j\bigg).
\end{aligned}$$

We evaluate the system (1) using the NSFD technique and the numerical values from [[37]] that are listed in 2.

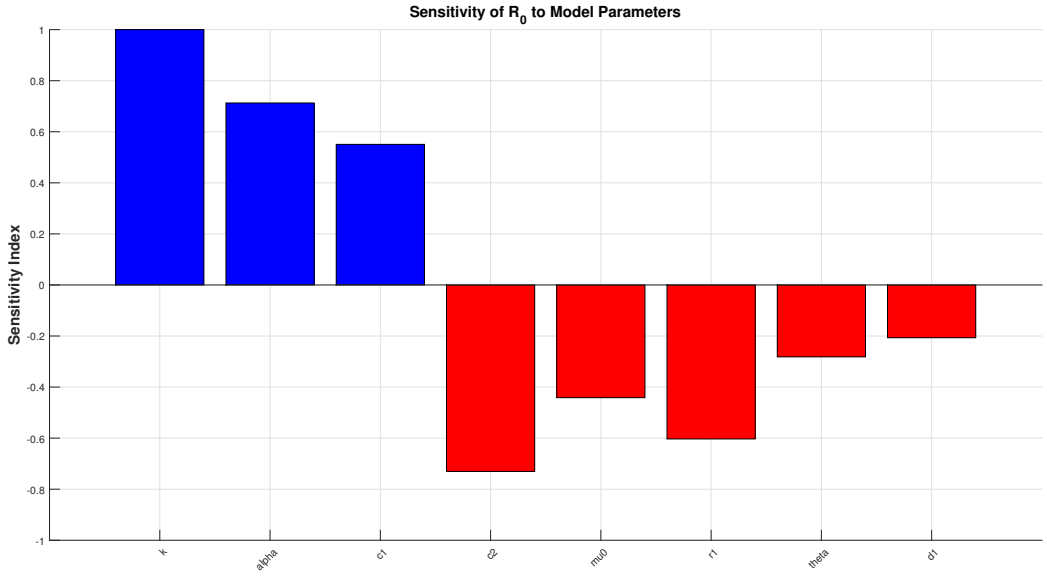

Figure 1: Sensitivity index.

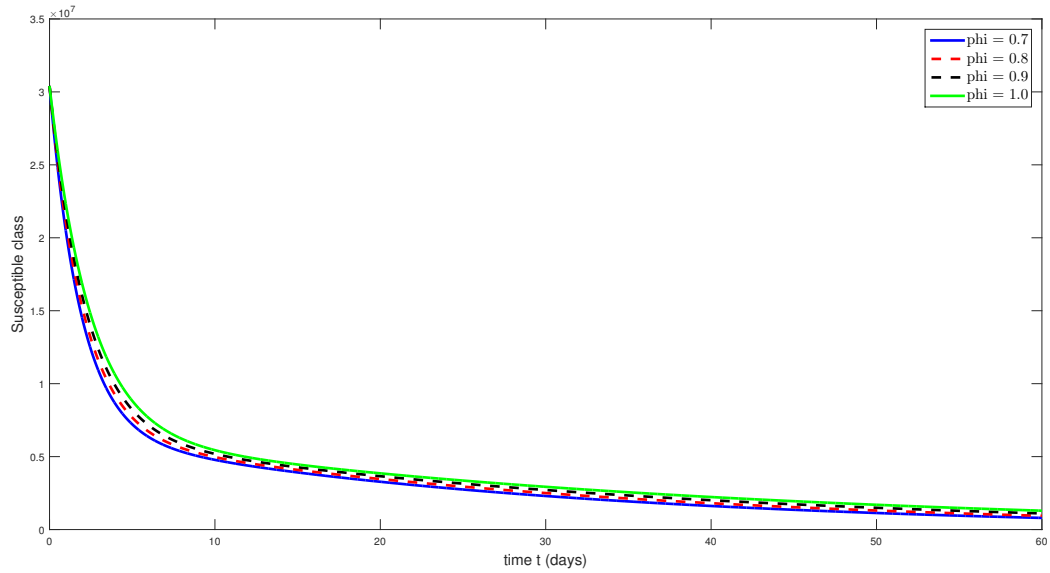

Figure 3: NSFD-based graph of computations for the deterministic model (1) susceptible compartment.

Variables	The Physical Representation	Values
b	The rate at which new population entered susceptible	0.0784
k	Infectious rate	0.9091
c_2	The rate of vaccinated population entered from $\mathbb{I}$ to $\mathbb{V}$	0.6
c_1	The rate of transmission of exposed population entered from $\mathbb{E}$ to $\mathbb{I}$	0.167
α	The rate of transmission of exposed population entered from $\mathbb{E}$ to $\mathbb{I}$	0.14286
θ	The rate of transmission of infected population entered from $\mathbb{I}$ to $\mathbb{T}$	0.03
r_2	The rate of transmission of treatments population entered from $\mathbb{T}$ to $\mathbb{R}$	0.125
r_1	The rate of transmission of self recovered population entered from $\mathbb{E}$ to $\mathbb{R}$	0.3425
d_1	Infectious death rate in $\mathbb{I}$	0.02202
d_2	Disease-related death rate in $\mathbb{T}$	0.0550
μ_0	Natural death rate	0.0545

Table 2: The parameters and their description involved in the model (1).

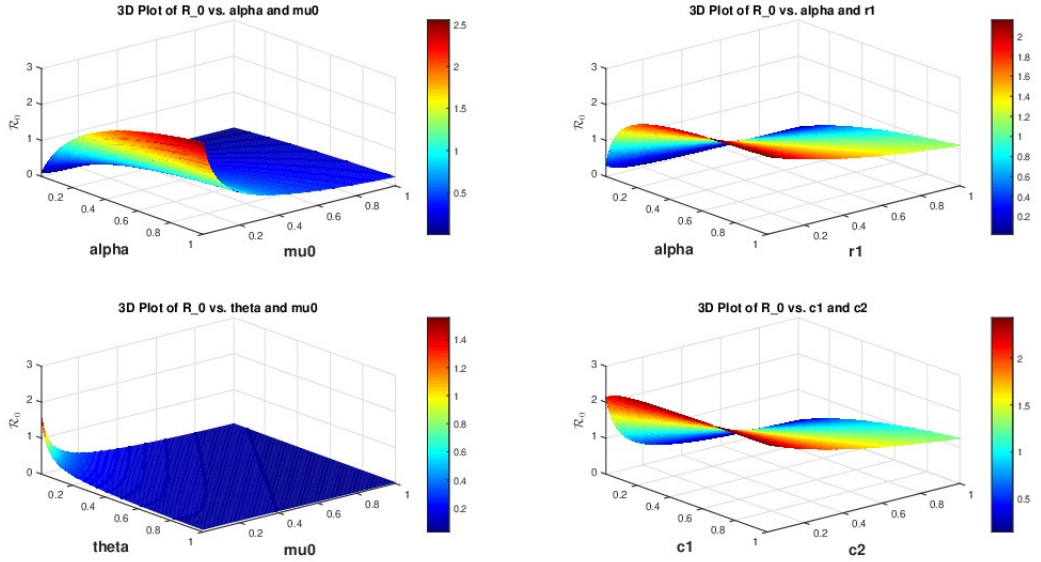

Figure 2: 3D dynamics of $\mathcal{R}_0$ of COVID-19n two strains with sensitive parameters.

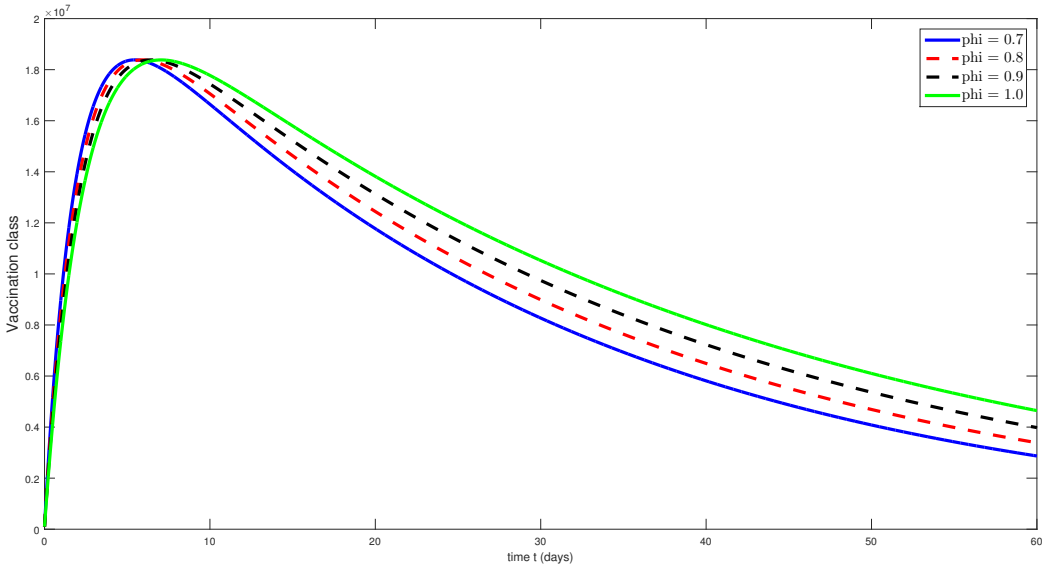

Figure 4: NSFD-based graph of computations for the deterministic model (1) vaccination compartment.

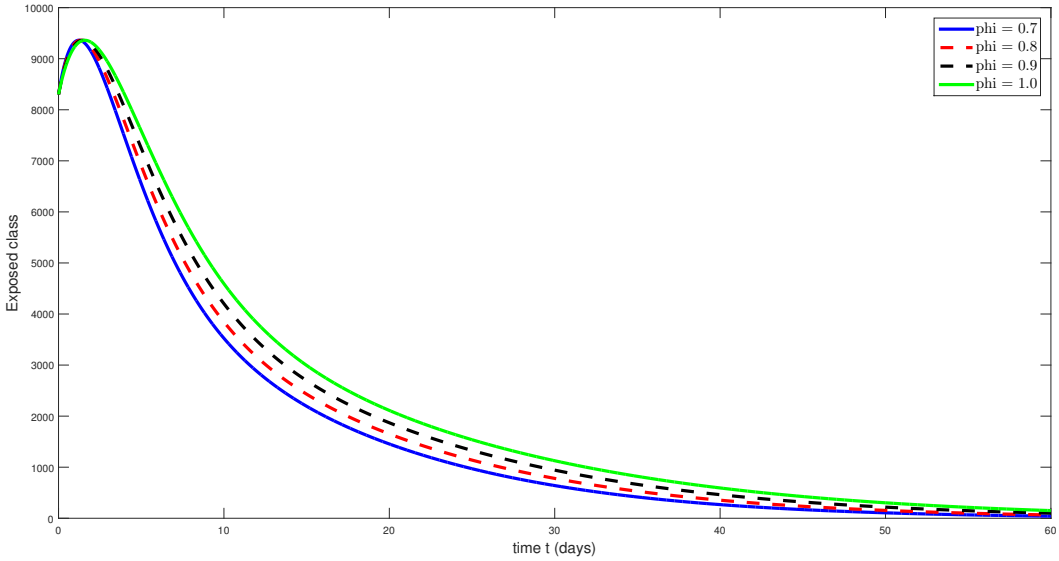

Figure 5: NSFD-based graph of computations for the deterministic model (1) exposed compartment.

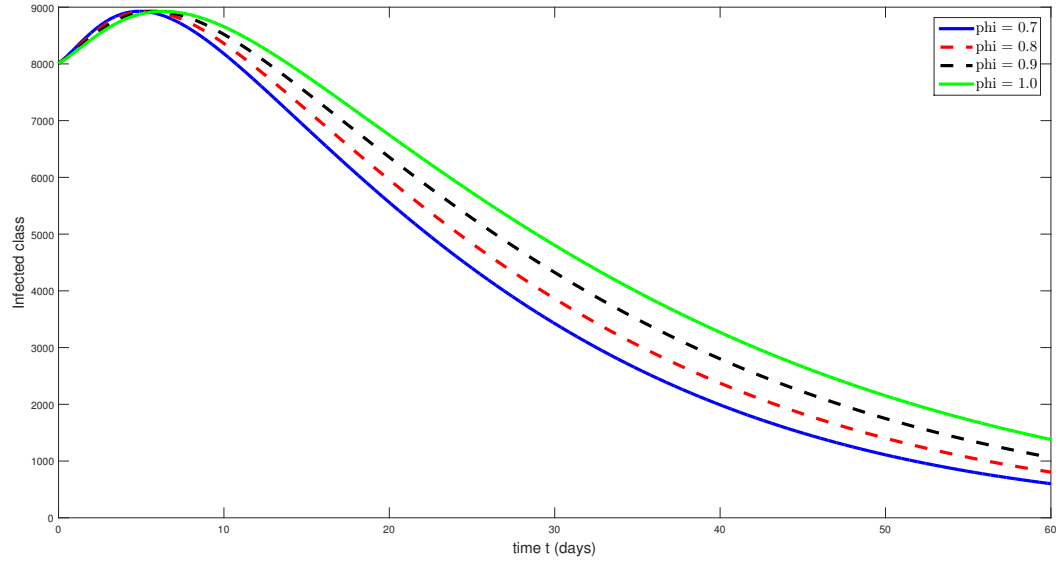

Figure 6: NSFD-based graph of computations for the deterministic model (1) infected compartment.

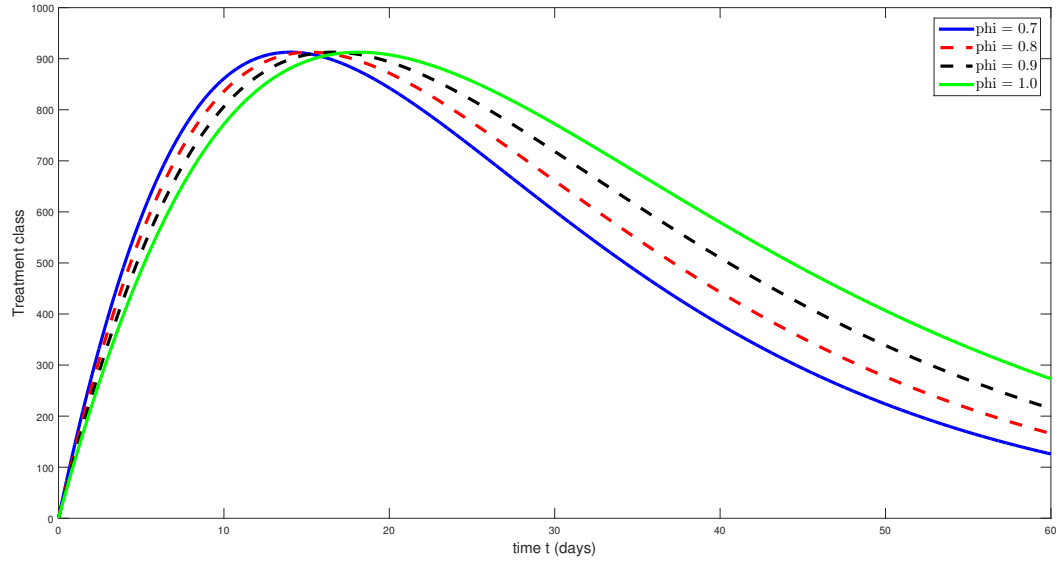

Figure 7: NSFD-based graph of computations for the deterministic model (1) treatment compartment.

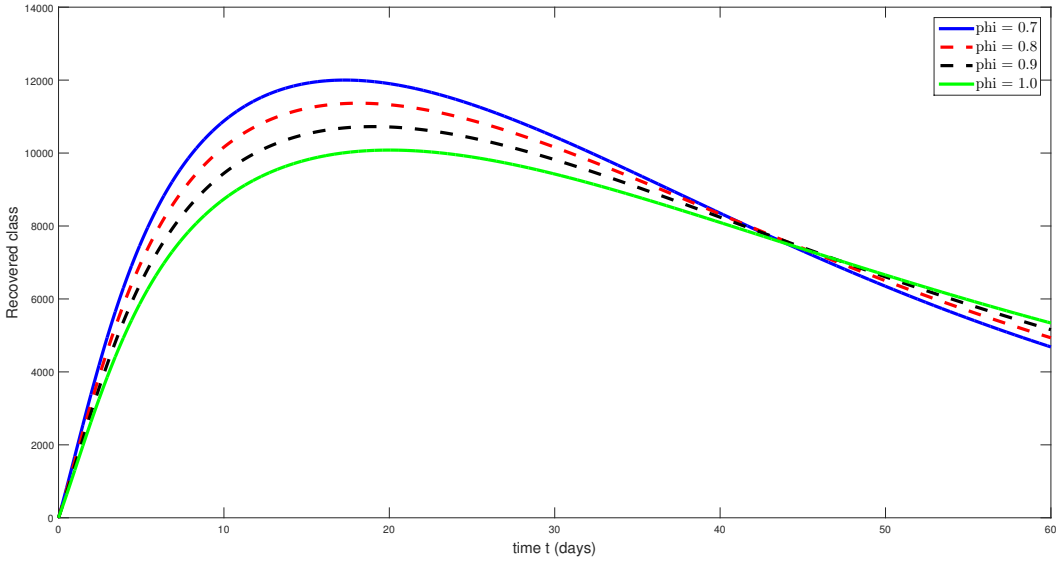

Figure 8: NSFD-based graph of computations for the deterministic model (1). recovered compartment

Using data from Table (1), we plotted the model through the NSFD scheme. From Figure (3), we observe that susceptibility decreases over time and stabilizes after about one month. Implementing a vaccination campaign before infection helps reduce the disease flow

and achieves satisfactory stability (see 4). In the absence of clear symptoms, populations are exposed to the disease, and the dynamics of the compartments are shown in Figure (5). Initially, the infection class is at a high level, but after treatment and the vaccination campaign, a decline in the disease flow is seen (see 6). Applying treatment strategies to control the disease, Figure (7) shows an exponential growth in the recovered compartment, demonstrating the model's accuracy and usefulness (see 8).

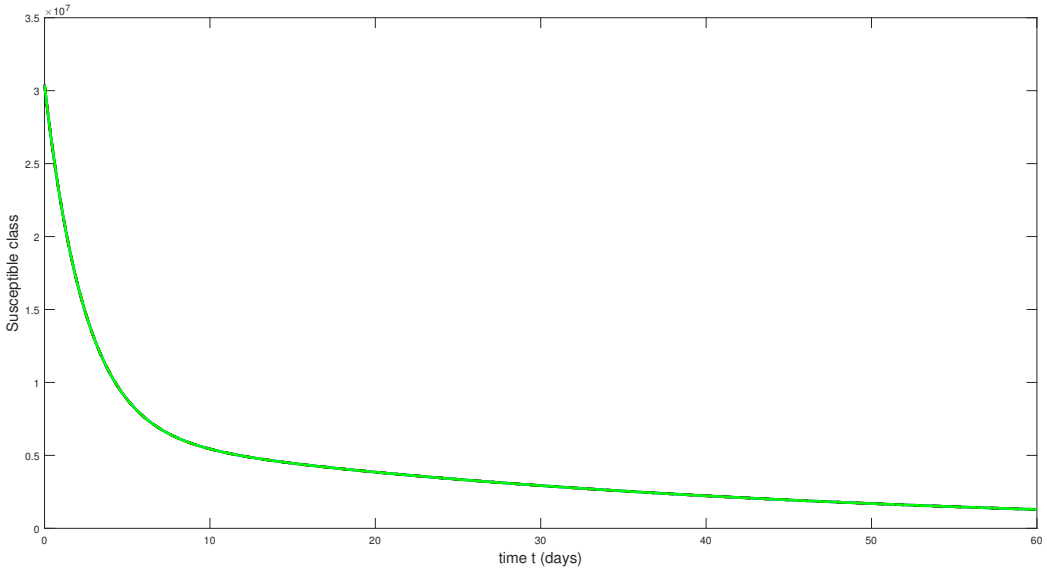

Figure 9: Plot of fractional technique based numerical solutions for the deterministic model (1) susceptible compartment.

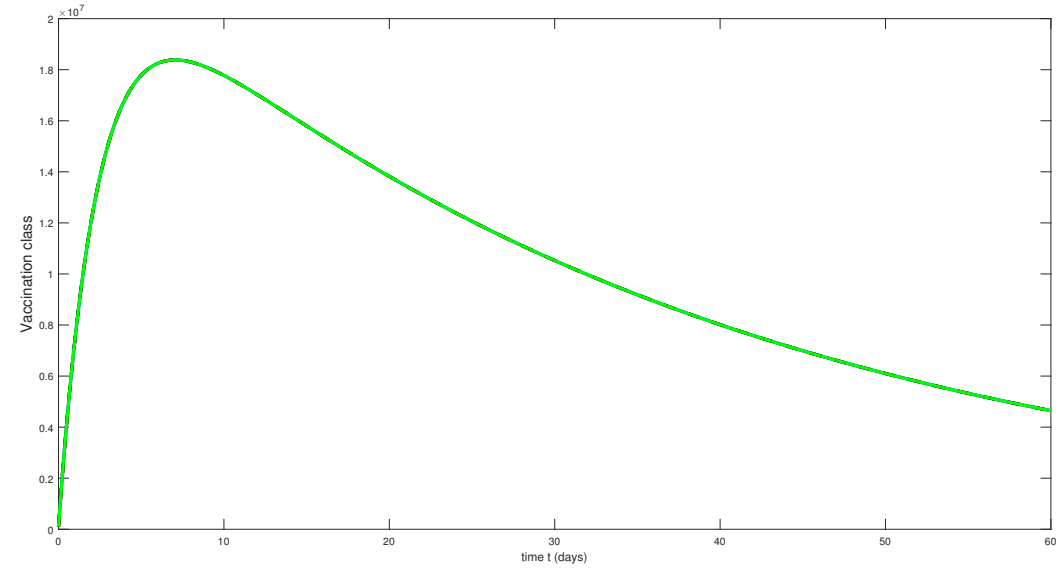

Figure 10: Plot of fractional technique-based numerical solutions for the deterministic model (1) vaccination compartment.

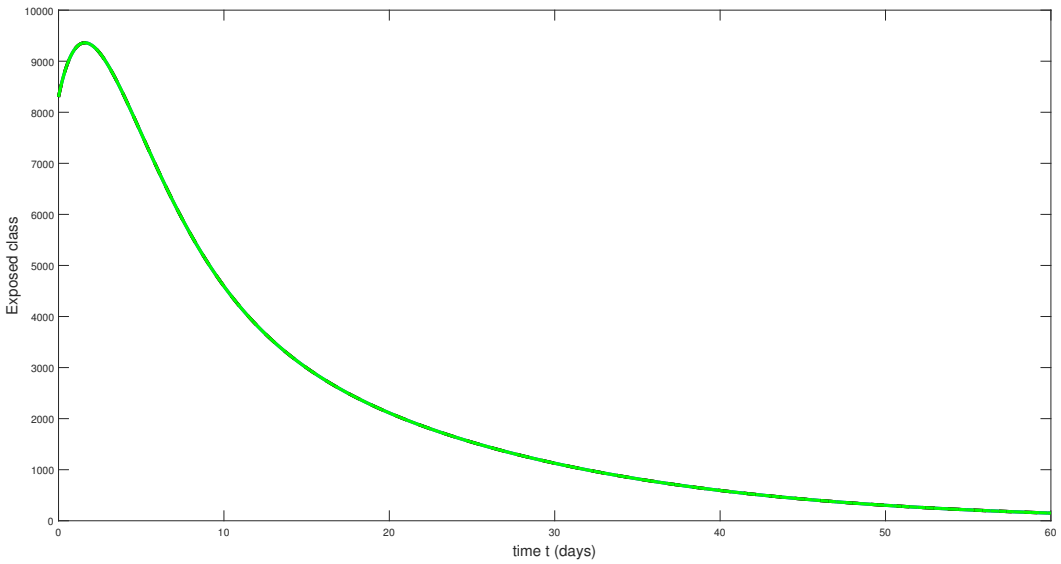

Figure 11: Plot of fractional technique-based numerical solutions for the deterministic model (1) (1) exposed compartment.

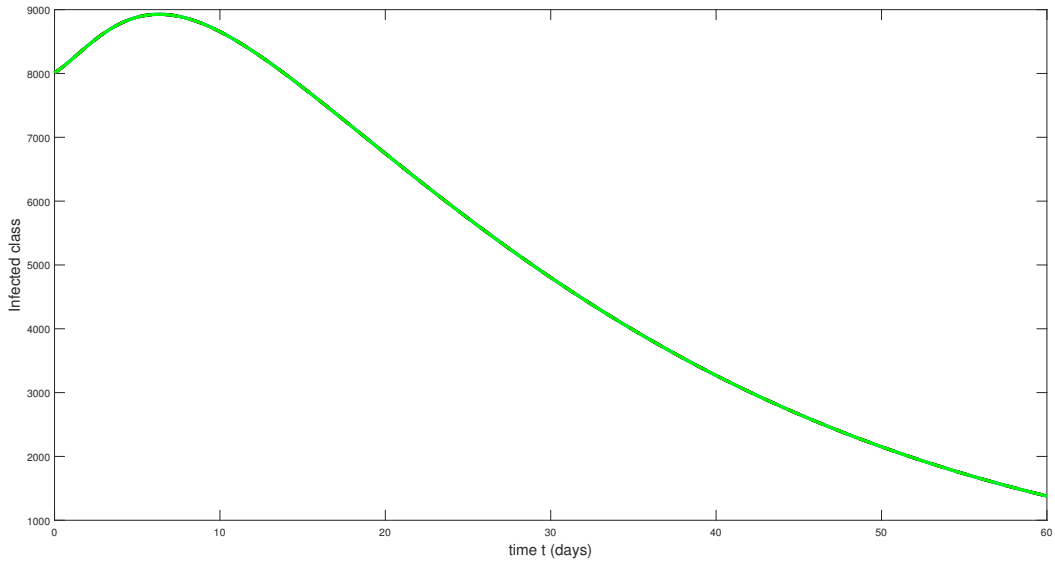

Figure 12: Plot of fractional technique-based numerical solutions for the deterministic model (1) (1) infected compartment.

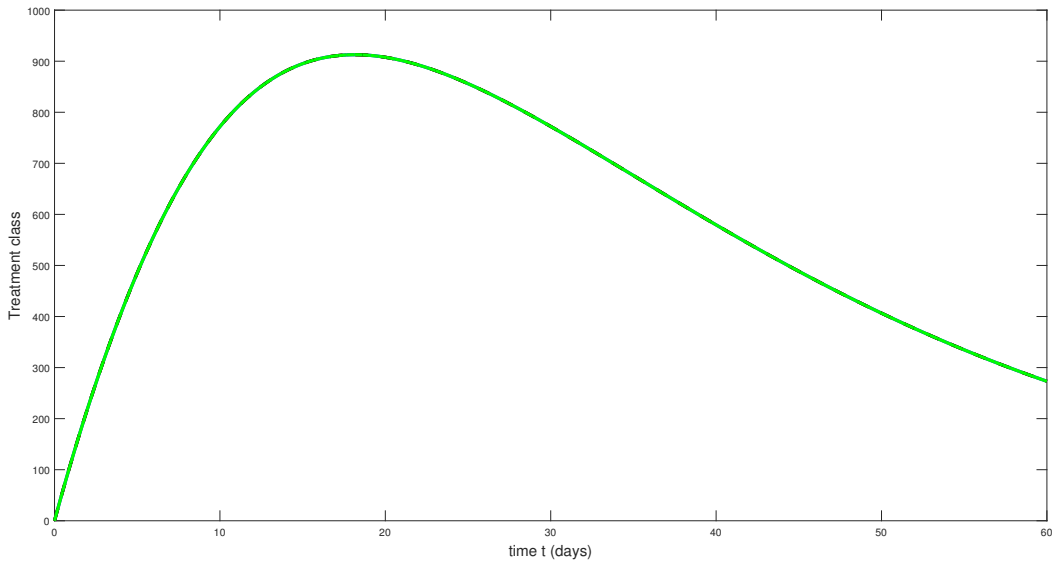

Figure 13: Plot of fractional technique-based numerical solutions for the deterministic model (1) (1) treatment compartment.

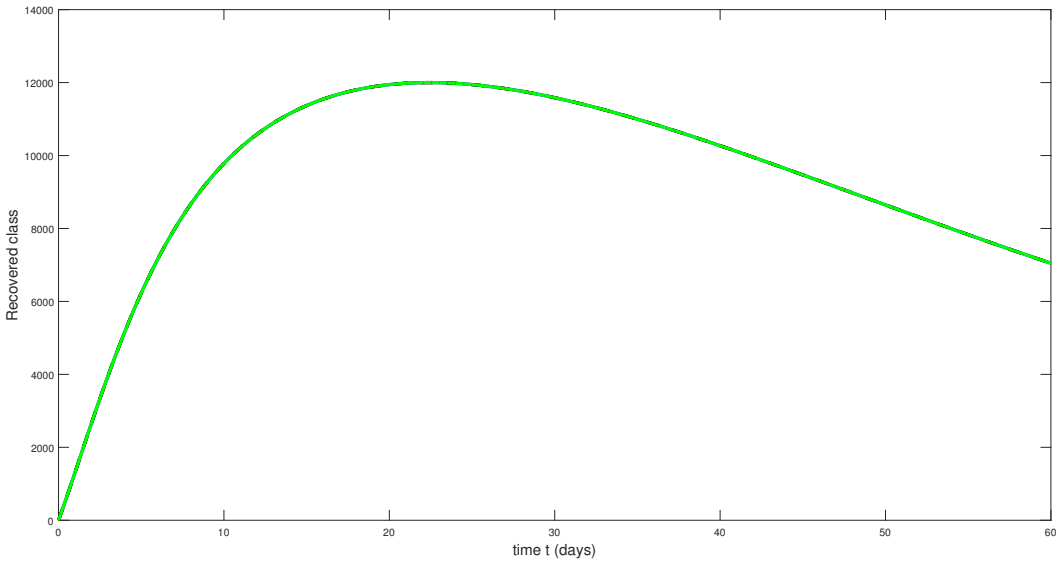

Figure 14: Plot of fractional technique-based numerical solutions for the deterministic model (1) (1) recovered compartment.

Here, we model the illness dynamics using the RK2 (second-order Runge-Kutta) fractional numerical technique. We illustrate the model using this approach, which entails gradually approximating the solution of the system of differential equations, using data from Table (1). Because it strikes a balance between precision and computing efficiency, the RK2 approach is frequently used in fractional systems. In figures (9-14), we plotted the system (1) using the fractional order $\alpha = 0.7, 0.8, 0.9, 1$.
As we can see from Figure (9), the population's susceptibility gradually declines and stabilizes after about a month, which is comparable to the outcomes of the NSFD scheme. But the RK2 approach captures these dynamics more accurately, particularly when it comes to fleeting behaviors. Once more, the stability attained here suggests that the disease's development has been successfully modeled.
A major factor in reducing the spread of disease is the introduction of a vaccination campaign prior to the commencement of infection, as shown in Figure (10). Over time, a more stable population results from the vaccination campaign's reduction of the number of vulnerable people and greater suppression of the disease flow. The consequences of the immunization campaign can be precisely recorded because to the RK2 scheme's ability to fine-tune these modifications. The number of exposed individuals declines over time under varying fractional order α values, as illustrated in figure (11). In contrast to greater values (e.g., 1.0), lower values of α (e.g., 0.7) cause a slower decline, suggesting that fractional-order models reflect memory effects that impact the course of disease. The decrease in the number of infected people over time is shown in figure (12), which shows a similar pattern. A slower decline occurs with a lower α, indicating that memory effects extend the population's infection period.

The number of people receiving therapy over time is depicted in figure (13). The number of people receiving treatment first increases, peaks, and then progressively decreases. Lower values of the fractional order α show a slower fall, indicating that treatment dynamics are influenced by memory effects. The model exhibits a more conventional integer-order trend with a quicker fall when $\alpha = 1.0$. The reconstructed population's dynamics throughout time are depicted in figure (14). As infected individuals recover, the number of recovered persons rises, peaking before leveling off. A longer-lasting memory impact in the system is suggested by a greater recovery peak at lower α values (e.g., 0.7). The typical integer-order model ($\alpha = 1.0$) exhibits a quicker stabilization and a somewhat lower peak.

8. The stochastic form of the model (1)

In this section, we incorporate the effect of atmospheric white noise by transforming the original deterministic eye disease system (1) into a stochastic system, as described in [38]. To achieve this, nonlinear perturbations are introduced into each equation of the system. Specifically, the rate of change is modified individually for each compartment to reflect the impact of stochastic fluctuations within that class.

$$\begin{aligned}
\mathbb{S}(t): \quad -c_1 &\longrightarrow \quad -\beta + (\Phi_{11}\mathbb{S} + \Phi_{12})\mathcal{B}_1(t),\\
\mathbb{V}(t): \quad -c_2 &\longrightarrow \quad -\mu + (\Phi_{21}\mathbb{V} + \Phi_{22})\mathcal{B}_2(t),\\
\mathbb{E}(t): \quad -\alpha &\longrightarrow \quad -\beta + (\Phi_{31}\mathbb{E} + \Phi_{32})\mathcal{B}_3(t),\\
\mathbb{I}(t): \quad -\theta &\longrightarrow \quad -\mu + (\Phi_{41}\mathbb{I} + \Phi_{42})\mathcal{B}_4(t),\\
\mathbb{T}(t): \quad -r_2 &\longrightarrow \quad -r + (\Phi_{51}\mathbb{T} + \Phi_{52})\mathcal{B}_5(t),\\
\mathbb{R}(t): \quad -\mu_0 &\longrightarrow \quad -d_0 + (\Phi_{61}\mathbb{R} + \Phi_{62})\mathcal{B}_6(t).
\end{aligned}$$

The following set of equations represents the stochastic form of system (1):

$$\begin{aligned}
d\mathbb{S} &= [b + c_1\mathbb{V} - \tfrac{k\mathbb{S}\mathbb{I}}{\mathbb{M}} - (c_2 + \mu_0)\mathbb{S}]dt + (\Phi_{11}\mathbb{S} + \Phi_{12})\mathbb{S}\, d\mathcal{B}_1(t),\\
d\mathbb{V} &= [c_2\mathbb{S} - (c_1 + \mu_0)\mathbb{V}]dt + (\Phi_{21}\mathbb{V} + \Phi_{22})\mathbb{V}\, d\mathcal{B}_2(t),\\
d\mathbb{E} &= [\tfrac{k\mathbb{S}\mathbb{I}}{\mathbb{M}} - (\alpha + r_1 + \mu_0)\mathbb{E}]dt + (\Phi_{31}\mathbb{E} + \Phi_{32})\mathbb{E}\, d\mathcal{B}_3(t),\\
d\mathbb{I} &= [\alpha\mathbb{E} - (\theta + d_1 + \mu_0)\mathbb{I}]dt + (\Phi_{41}\mathbb{I} + \Phi_{42})\mathbb{I}\, d\mathcal{B}_4(t),\\
d\mathbb{T} &= [\theta\mathbb{I} - (r_2 + d_2 + \mu_0)\mathbb{T}]dt + (\Phi_{51}\mathbb{T} + \Phi_{52})\mathbb{T}\, d\mathcal{B}_5(t),\\
d\mathbb{R} &= [r_2\mathbb{T} + r_1\mathbb{E} - \mu_0\mathbb{R}]dt + (\Phi_{61}\mathbb{R} + \Phi_{62})\mathbb{R}\, d\mathcal{B}_6(t).
\end{aligned} \tag{27}$$

We are now present the numerical simulation of this stochastic model in the next section.

9. Stochastic model (27) numerical analysis

Using the Euler-Maruyama approach, the trajectories or approximated solutions of a stochastic system problem are found using the following equation:

$$\chi_{t_{i+1}} = \chi_{t_i} + \alpha(t_i, \chi_{t_i}) + \beta(t_i, \chi_{t_i})\Delta A_i. \tag{28}$$

The case where $i = 0, 1, ..., n-1$. Comprehending the computation of ΔA_i is necessary for the computational implementation of the process. instances in which $i = 0, 1, ..., n-1$. The computer implementation of the procedure requires an understanding of how to compute of ΔA_i. Suppose that η is a random variable with an average $\eta \sim M(0, 1)$. A normal distribution is thus indicated by $\sqrt{\Delta t}\eta_1$ with zero mean and variance Δt, that is, $\sqrt{\Delta t}\eta_1 \sim M(0, \Delta t)$. The system of dynamic differential equations (27) must be appropriately separated for our suggested model in order to apply the Euler-Maruyama approach method similarly (28). This can be done by

$$\begin{aligned}
\mathbb{S}_{t_{i+1}} &= \mathbb{S}_{t_i} + \left[b + c_1\mathbb{V} - \frac{k\mathbb{S}\mathbb{I}}{\mathbb{M}} - (c_2 + \mu_0)\mathbb{S}\right]\Delta t + \sqrt{\Delta t}\eta_1, \\
\mathbb{V}_{t_{i+1}} &= \mathbb{V}_{t_i} + [c_2\mathbb{S} - (c_1 + \mu_0)\mathbb{V}]\,\Delta t + \sqrt{\Delta t}\eta_2, \\
\mathbb{E}_{t_{i+1}} &= \mathbb{E}_{t_i} + \left[\frac{k\mathbb{S}\mathbb{I}}{\mathbb{M}} - (\alpha + r_1 + \mu_0)\mathbb{E}\right]\Delta t + \sqrt{\Delta t}\eta_3, \\
\mathbb{I}_{t_{i+1}} &= \mathbb{I}_{t_i} + [\alpha\mathbb{E} - (\theta + d_1 + \mu_0)\mathbb{I}]\,\Delta t + \sqrt{\Delta t}\eta_4, \\
\mathbb{T}_{t_{i+1}} &= \mathbb{T}_{t_i} + [\theta\mathbb{I} - (r_2 + d_2 + \mu_0)\mathbb{T}]\Delta t + \sqrt{\Delta t}\eta_5, \\
\mathbb{R}_{t_{i+1}} &= \mathbb{R}_{t_i} + [r_2\mathbb{T} + r_1\mathbb{E} - \mu_0\mathbb{R}]\Delta t + \sqrt{\Delta t}\eta_6.
\end{aligned} \tag{29}$$

Using this numerical scheme, we compare with NSFD scheme in next figures.

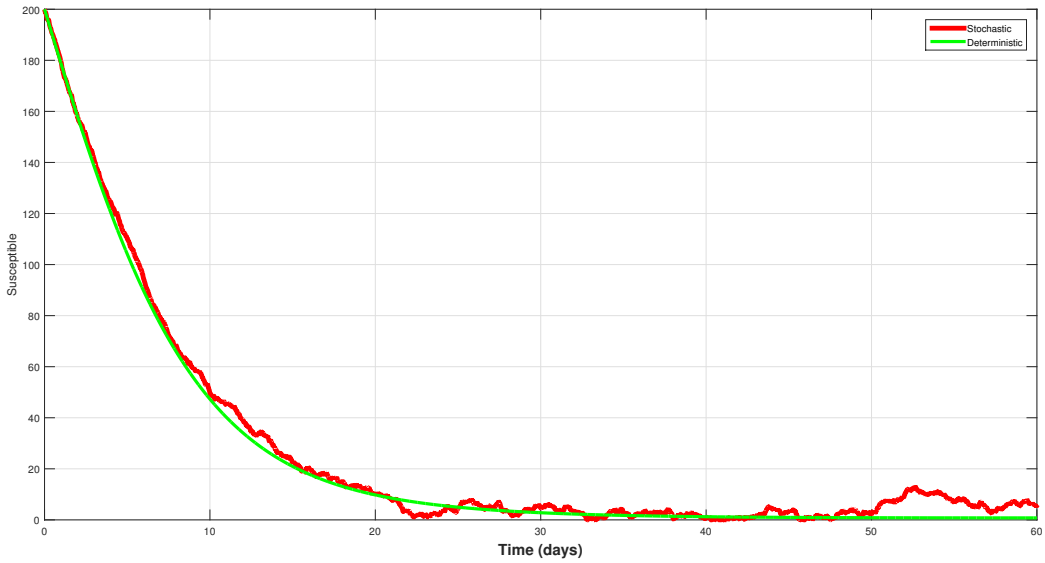

Figure 15: Comparison of stochastic and deterministic model (1) susceptible compartment $\mathbb{S}$.

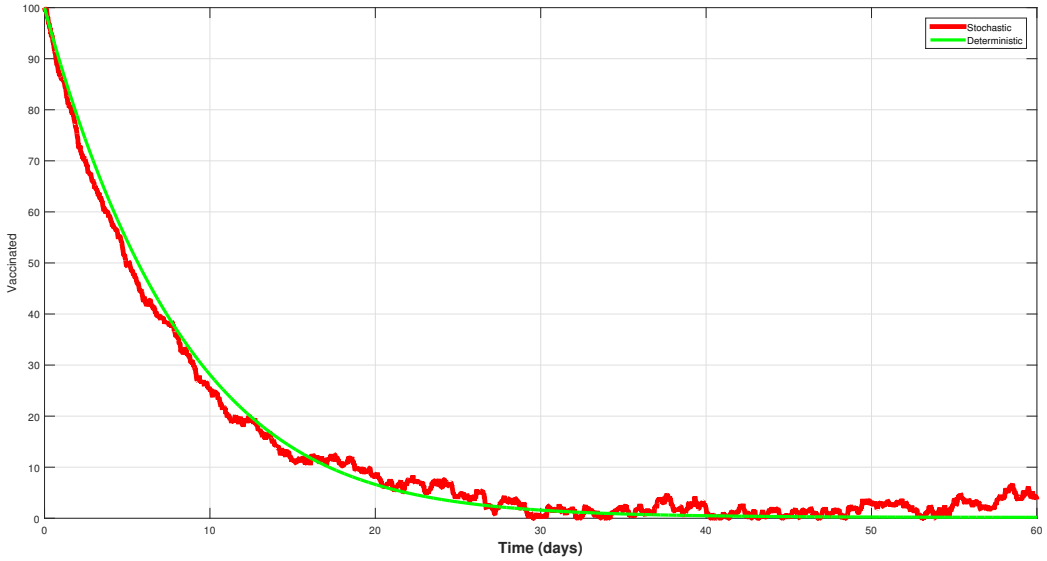

Figure 16: Comparison of stochastic and deterministic model (1) vaccination compartment $\mathbb{V}$.

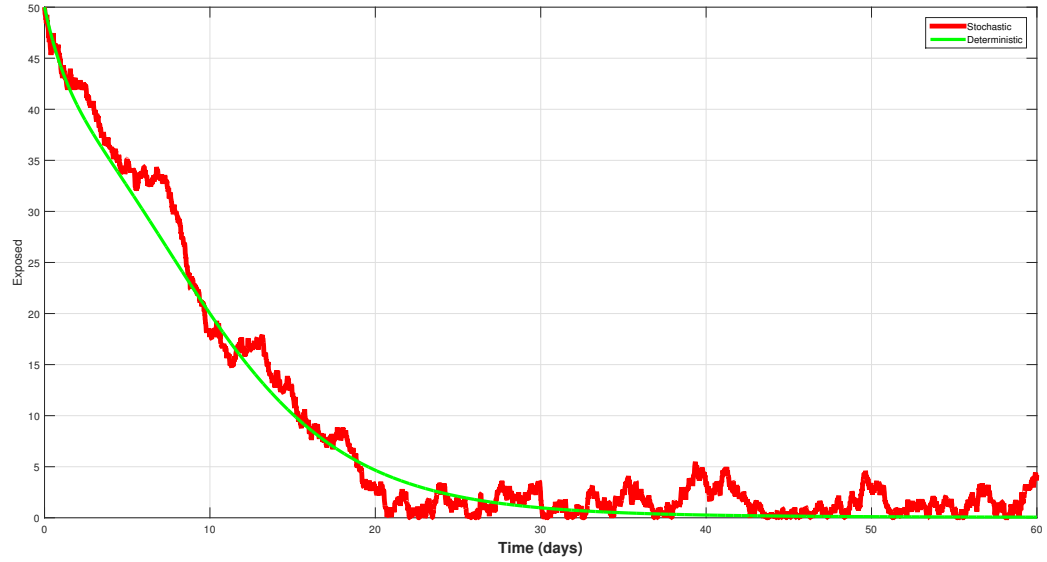

Figure 17: Comparison of stochastic and deterministic model (1) exposed compartment $\mathbb{E}$.

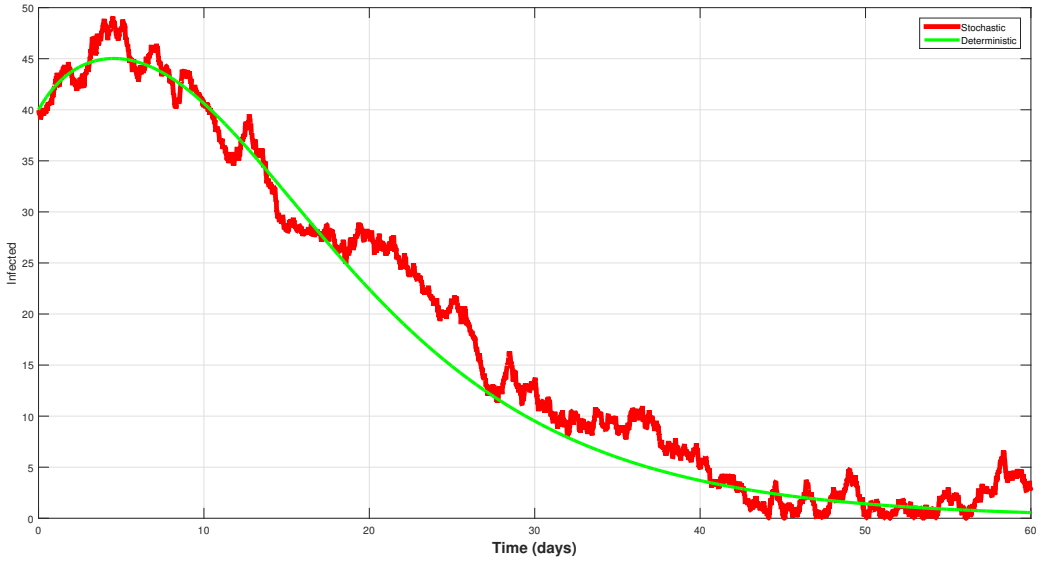

Figure 18: Comparison of stochastic and deterministic model (1) infected compartment $\mathbb{I}$.

Figure 19: Comparison of stochastic and deterministic model (1) treatment compartment $\mathbb{T}$.

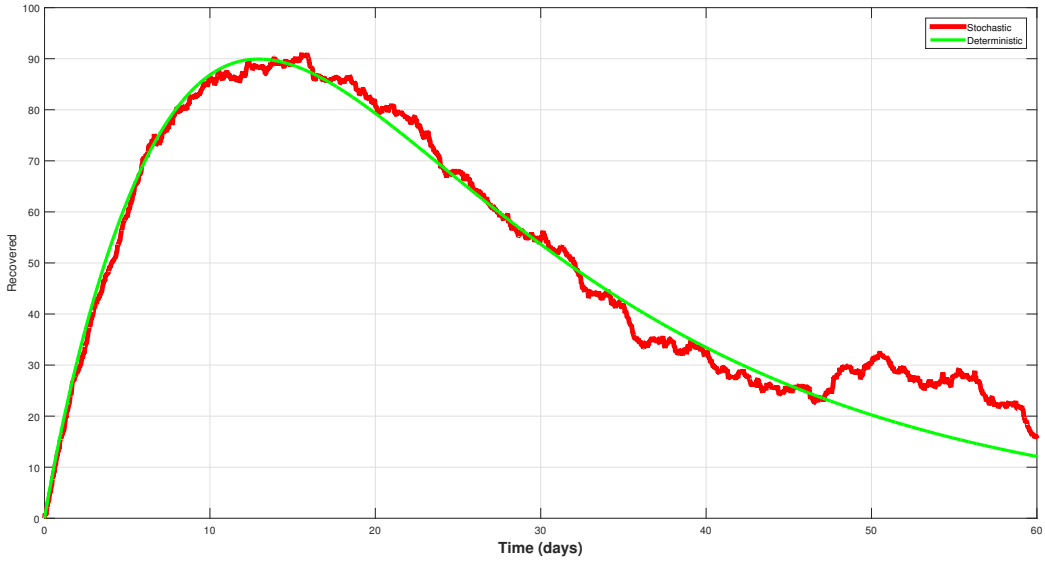

Figure 20: Comparison of stochastic and deterministic model (1) recovered compartment $\mathbb{R}$.

10. Conclusion

This paper develops an $SVEITR$ epidemiological model to investigate the dynamic movements of a novel of measles. By demonstrating the uniqueness and existences of a positively boundness of solution, we were able to demonstrate the dynamical system's epidemiological significance and establish the problem's well-posedness. The dynamic behavior of the suggested model at its equilibrium states was assessed through analytical calculation of the threshold parameter. This threshold value, which denotes circumstances under which the disease may either continue or disappear, was an essential indicator in epidemic modeling. Furthermore local and global unsteady equilibrium stabilities of the solutions were established by applying the necessary constraints on the threshold value. The global consistency of states of equilibrium was demonstrated using the Lyapunov function theory. The statistical dynamics of viral disease were investigated in detail using the NSFD numerical scheme, which was found to be compatible with the continuum model. The purpose of the study was to find out how well continuous treatment and immunization control strategies, which don't change over time, can stop the spread of measles. The findings suggest that raising vaccination rates may lower the number of infectious cases and, if not less than 40% of the vulnerable population receives the shot, may even eradicate measles.

Furthermore, increasing the rate of treatment can also help stop the transmission of measles because higher treatment levels result in a small increase in the vulnerable population but a decrease in the total number of infected people. It was determined that in addition to vaccination, therapy is helpful. According to the research, if at least 15% of

affected people receive treatment, it is possible to eradicate disease from human beings once vaccination is accessible. All things considered, when combined, a comprehensive approach that includes vaccination a sizable percentage of vulnerable people, attaining as many as forty percent, and treating not less than 15% of the sick population can be quite successful in preventing measles. This joint strategy seeks to reduce infections, lessen the disease's severity, and enhance general public health results. Evaluating the sensitivity of variables influencing a threshold factor in the proposed Measles model was the main goal of our investigation. A rate of contact k of susceptible and infected people was found to be the most significant parameter. Educating and organizing people who can act as advocates and increase public awareness is essential. These powerful people will be essential in motivating others to investigate various approaches meant to reduce transmission rates. They can significantly help reduce the virus's transmission by promoting preventive measures like social distance, vitamin A supplementation (particularly in youngsters), and adherence to good hygiene standards. These people's awareness efforts will inspire the public to think creatively and proactively about other ways to reduce transmission rates. The aim of the mathematical analysis conducted in the present research was to gain a full understanding of the long-term evolution of measles. We think that those making decisions and health authorities will find the knowledge gathered from this study to be helpful in the fight against measles. Subsequent studies will examine general fractional and stochastic optimum control problems using actual data in order to identify the best controls for putting required measures into place.

Acknowledgements

The authors would like to acknowledge the support of Prince Sultan University for paying the Article Processing Charges (APC) of this publication.
Declarations All authors have read and approved the final manuscript.
Competing interests Not exist.

References

[1] Shinjini Bandopadhyay, Angana Das Gupta, Asesh Banerjee, and Prabuddha Gupta. Bitesize epidemiology for general awareness of all students-i. *Resonance*, 28(3):411–432, 2023.

[2] UNICEF, WHO, et al. Who warn of perfect storm of conditions for measles outbreaks, affecting children. *New York: Organización Mundial de la Salud*, 2022.

[3] Babatunde Sunday Ogundare and James Akingbade. Boundedness and stability properties of solutions of mathematical model of measles. *Tamkang Journal of Mathematics*, 52(1):91–112, 2021.

[4] Bing Guo, Asad Khan, and Anwarud Din. Numerical simulation of nonlinear stochastic analysis for measles transmission: A case study of a measles epidemic in pakistan. *Fractal and Fractional*, 7(2):130, 2023.

[5] Mamadou L. Diagne, Herieth Rwezaura, Sansao A. Pedro, and Jean M. Tchuenche. Theoretical analysis of a measles model with nonlinear incidence functions. *Communications in Nonlinear Science and Numerical Simulation*, 117:106911, 2023.

[6] Ryoko Sato and Masahiko Haraguchi. Effect of measles prevalence and vaccination coverage on other disease burden: Evidence of measles immune amnesia in 46 african countries. *Human Vaccines & Immunotherapeutics*, 17(12):5361–5366, 2021.

[7] Siwaphorn Kanchanarat, Kadkanok Nudee, Settapat Chinviriyasit, and Wirawan Chinviriyasit. Mathematical analysis of pulse vaccination in controlling the dynamics of measles transmission. *Infectious Disease Modelling*, 8(4):964–979, 2023.

[8] Getachew Teshome Tilahun, Seleshi Demie, and Alemayehu Eyob. Stochastic model of measles transmission dynamics with double dose vaccination. *Infectious Disease Modelling*, 5:478–494, 2020.

[9] Anjana Pokharel, Khagendra Adhikari, Ramesh Gautam, Kedar Nath Uprety, and Naveen K. Vaidya. Modeling transmission dynamics of measles in nepal and its control with monitored vaccination program. *Mathematical Biosciences and Engineering*, 19(8), 2022.

[10] David Nuwahereze, Martins Onyekwelu Onuorah, Baba Mohammed Abdulahi, and Innocent Kabandana. Standard incidence model of measles with two vaccination strategies. *World Scientific News*, 170:149–171, 2022.

[11] Muhammad Fakhruddin, Dani Suandi, H. Fahlena Sumiati, Nuning Nuraini, and Edy Soewono. Investigation of a measles transmission with vaccination: A case study in jakarta, indonesia. *Mathematical Biosciences and Engineering*, 17(4):2998–3018, 2020.

[12] Dipo Aldila and Dinda Asrianti. A deterministic model of measles with imperfect vaccination and quarantine intervention. In *Journal of Physics: Conference Series*, volume 1218, page 012044. IOP Publishing, 2019.

[13] Sarah Thompson, Johanna C. Meyer, Rosemary J. Burnett, and Stephen M. Campbell. Mitigating vaccine hesitancy and building trust to prevent future measles outbreaks in england. *Vaccines*, 11(2):288, 2023.

[14] W. Ahmad, A. I. K. Butt, M. Rafiq, Z. Asif, T. Ismaeel, and N. Ahmad. Modeling, analyzing and simulating the measles transmission dynamics through efficient computational optimal control technique. *The European Physical Journal Plus*, 139(7):1–30, 2024.

[15] Goodluck Nchasi, Innocent Kitandu Paul, Sospeter Berling Sospeter, Margareth Richard Mallya, Juvenali Ruaichi, and Johnson Malunga. Measles outbreak in sub-saharan africa amidst covid-19: A rising concern, efforts, challenges, and future recommendations. *Annals of Medicine and Surgery*, 81, 2022.

[16] Shinta A. Rahmayani, Dipo Aldila, and Bevina D. Handari. Cost-effectiveness analysis on measles transmission with vaccination and treatment intervention. *AIMS Mathematics*, 6(11):12491–12527, 2021.

[17] Yuyi Xue, Xiaoe Ruan, and Yanni Xiao. Measles dynamics on network models with optimal control strategies. *Advances in Difference Equations*, 2021(1):138, 2021.

[18] Ratchada Viriyapong and Witchaya Ridbamroong. Global stability analysis and op-

timal control of measles model with vaccination and treatment. *Journal of Applied Mathematics and Computing*, 62(1):207–237, 2020.

[19] Dani Suandi. Optimal control problem of vaccination for the spread of measles diseases model. *Jurnal Riset Dan Aplikasi Matematika (JRAM)*, 2(2):76–83, 2018.

[20] Md Abdul Kuddus, Azizur Rahman, Farzana Alam, and M. Mohiuddin. Analysis of the different interventions scenario for programmatic measles control in bangladesh: A modelling study. *PLoS One*, 18(6):e0283082, 2023.

[21] Hailay Weldegiorgis Berhe and Oluwole Daniel Makinde. Computational modelling and optimal control of measles epidemic in human population. *Biosystems*, 190:104102, 2020.

[22] S. O. Adewale, I. A. Olopade, S. O. Ajao, and G. A. Adeniran. Optimal control analysis of the dynamical spread of measles. *International Journal of Research-GRANTHAALAYAH*, 2016.

[23] Chinwendu E. Madubueze, Isaac O. Onwubuya, and Iorwuese Mzungwega. Controlling the transmission dynamics of measles infection: Sensitivity analysis and optimal control analysis approaches. *Ratio Mathematica*, 43:41–63, 2022.

[24] Peijiang Liu, Rukhsar Ikram, Amir Khan, and Anwarud Din. The measles epidemic model assessment under real statistics: An application of stochastic optimal control theory. *Computer Methods in Biomechanics and Biomedical Engineering*, 26(2):138–159, 2023.

[25] Israr Ahmad, Zeeshan Ali, Babar Khan, Kamal Shah, and Thabet Abdeljawad. Exploring the dynamics of gumboro-salmonella co-infection with fractal fractional analysis. *Alexandria Engineering Journal*, 117:472–489, 2025.

[26] Mdi Begum Jeelani, Abeer S. Alnahdi, Rahim Ud Din, Hussam Alrabaiah, and Azeem Sultana. Mathematical model to investigate transmission dynamics of covid-19 with vaccinated class. *AIMS Mathematics*, 8(12):29932–29955, 2023.

[27] M. Lau and Z. G. Arenas. Stochastic modeling of a measles outbreak in brazil. *Trends in Computational and Applied Mathematics*, 24(3):459–473, 2023.

[28] Muhammad Riaz, Zeeshan Ali, Rahim Ud Din, Sadique Ahmad, Kamaleldin Abodayeh, and Muhammad Sarwar. Mathematical modeling with two strains to investigate evolution of covid-19 from computational and theoretical perspectives. *European Journal of Pure and Applied Mathematics*, 18(2):6001–6001, 2025.

[29] Haileyesus Tessema Alemneh and Asnakew Mesele Belay. Modelling, analysis, and simulation of measles disease transmission dynamics. *Discrete Dynamics in Nature and Society*, 2023(1):9353540, 2023.

[30] Olumuyiwa James Peter, Hasan S. Panigoro, Mahmoud Abdalla Ali Ibrahim, Olusegun Michael Otunuga, Tawakalt Abosede Ayoola, and Asimiyu Olalekan Oladapo. Analysis and dynamics of measles with control strategies: A mathematical modeling approach. *International Journal of Dynamics and Control*, 11(5):2538–2552, 2023.

[31] Kamal Shah, Khalil UR Rehman, Bahaaeldin Abdalla, Thabet Abdeljawad, and Wasfi Shatanawi. Using neural network and fractals fractional analysis to predict the eye disease infection caused by conjunctivitis virus. *Fractals*, page 2540204, 2025.

[32] Miled El Hajji and Amer Hassan Albargi. A mathematical investigation of an sveir

epidemic model for the measles transmission. *Mathematical Biosciences and Engineering*, 19(3):2853–2875, 2022.

[33] W. Ahmad, A. I. K. Butt, M. Rafiq, Z. Asif, T. Ismaeel, and N. Ahmad. Modeling, analyzing and simulating the measles transmission dynamics through efficient computational optimal control technique. *The European Physical Journal Plus*, 139(7):1–30, 2024.

[34] Meredith G. Dixon. Progress toward regional measles elimination worldwide, 2000–2020. *MMWR. Morbidity and Mortality Weekly Report*, 70, 2021.

[35] Paul A. Gastanaduy, Emily Banerjee, Chas DeBolt, Pamela Bravo-Alcántara, Samia A. Samad, Desiree Pastor, Paul A. Rota, Manisha Patel, Natasha S. Crowcroft, and David N. Durrheim. Public health responses during measles outbreaks in elimination settings: Strategies and challenges. *Human Vaccines & Immunotherapeutics*, 14(9):2222–2238, 2018.

[36] Md Rafiul Islam, Angela Peace, Daniel Medina, and Tamer Oraby. Integer versus fractional order seir deterministic and stochastic models of measles. *International Journal of Environmental Research and Public Health*, 17(6):2014, 2020.

[37] Rahim Ud Din, Khalid Ali Khan, Ahmad Aloqaily, Nabil Mlaiki, and Hussam Alrabaiah. Using non-standard finite difference scheme to study classical and fractional order seivr model. *Fractal and Fractional*, 7(7):2504–3110, 2023.

[38] Abdon Atangana and Seda İğret Araz. Modeling and forecasting the spread of covid-19 with stochastic and deterministic approaches: Africa and europe. *Advances in Difference Equations*, 2021(1):57, 2021.